THE AMERICAN MINERALOGIST
JOURNAL OF THE MINERALOGICAL SOCIETY OF AMERICA

Vol. 23 AUGUST, 1938 No. 8

DATA FOR THE CONSTRUCTION OF MODELS ILLUSTRATING THE ARRANGEMENT AND PACKING OF ATOMS IN CRYSTALS

(FORMULA TYPES A, AB, AND AB_2)

M. J. BUERGER AND ROBERT D. BUTLER,
Massachusetts Institute of Technology, Cambridge, Massachusetts, and Lehigh University, Bethlehem, Pennsylvania.

INTRODUCTION

In a recent paper,[1] the writers have presented a technique for the construction of models illustrating both the arrangement and the packing of atoms in crystals. Models of some sixty-odd crystal structure types have been constructed by the methods discussed. In most of the structure types, the positions of the atoms are sufficiently general to require a very considerable expenditure of effort in the several calculations necessary before an acceptable model can be constructed. The present paper gives the results of such calculations as have been made to date for certain simple structures. A later paper will present data for more complex structures.[2] Those wishing to duplicate such models may utilize the data herewith presented and proceed with the construction without further calculation.

As discussed in the first paper, certain relatively minor parameter adjustments have been made in almost all cases. For the benefit of those wishing to ascertain to what extent these minor changes have affected the accuracy of representing the actual crystal structure, the adjustments are outlined for each model.

The drilling coördinates could be best presented by a series of labelled plan views of the atoms in question, similar to figures 5 and 8 of the original paper. In order to save expense, however, a tabular method of presentation has been adopted. This lists for each ball the ρ and ϕ co-

[1] Buerger, M. J., and Butler, R. D., A technique for the construction of models illustrating the arrangement and packing of atoms in crystals: *Am. Mineral.*, vol. **21**, pp. 150–172, 1936.

[2] Data have already been published for models of some of the silicates: Dorris, J. E., Frondel, Clifford, Güssow, W. C., Lopez, V. M., Lord, C. S., Parrish, William and Shimer, J. A., Atomic packing models of some common silicate structures: *Am. Mineral.*, vol. **23**, pp. 65–84, 1938.

ordinates of each hole to be drilled, the ball to which the bond from each hole extends, and the key coördinate of the hole in the neighboring ball to which the bond extends. The latter facilitates orientation during construction. The number of balls of each kind required for a model is also given in the tabulation. The column presenting this is headed "Number of balls required for one unit cell model." In this case, a "one unit cell model" contains the atomic contents of one unit cell plus certain extra atoms. The latter are usually required to give mechanical support or rigidity to the cell contents, or are desirable in order to fill out the environment of the atoms in the cell. The designations "F" and "C" refers to models based upon face-centered and C-centered cells. They have been used where the smallest unit cell shows too little of the structure to be representative. Among hexagonal crystals, the designation "hex" indicates that the model contains 3 diamond-shaped hexagonal cell units, arranged to display the hexagonal symmetry of the model.

Under the discussion for each structure is given the source of the data used by the writers. This is not necessarily the publication of the original worker, as many of the data have been compiled in the standard reference works: *Struckturbericht*[3,4,5,6] I, II, III, and IV, (briefly referred to as S_I, S_{II}, S_{III} and S_{IV}), Wyckoff's *The Structure of Crystals*[7] (briefly referred to as W), Wyckoff's *Supplement*[8] (briefly referred to as WS) and Bragg's *The Atomic Structure of Minerals*[9] (briefly referred to as B).

The space group of the structures is also given, for even if the reference showing the general plan of the structure is not available, it is possible to construct models from a knowledge of the drilling coördinates and space group. It is advisable, however, to have a sketch or drawing of the structure to facilitate construction.

Ball sizes are suggested based upon the scale used by the writers, $1'' = 2$Å. Since the publication of the earlier paper, wooden balls have become available from the same source in diameter intervals of $1/16''$. Better representation of atomic sizes is now attained due to the availability of the intermediate sizes.

Where an easy construction scheme has been found for a model it is briefly described.

[3] Ewald, P. P., and Hermann, C., *Strukturbericht:* **1913–1928,** Leipzig (1931).

[4] Hermann, C., Lohrmann, O., and Philipp, H.: *Strukturbericht*, Band II, **1928–1932,** Leipzig (1937).

[5] Gottfried, C., and Schossberger, F.: *Strukturbericht*, Band III, **1933–1935,** Leipzig (1937).

[6] Gottfried, C.: *Strukturbericht*, Band IV, **1936,** Leipzig (1938).

[7] Wyckoff, Ralph W. G., *The structure of crystals*, 2nd ed., New York, **1931.**

[8] Wyckoff, Ralph W. G., *The structure of crystals; Supplement for* 1931–1934 *to the 2nd ed.*, New York, **1935.**

[9] Bragg, W. L., *Atomic structure of minerals.* Ithaca, **1937.**

Models for all known mineral structural types in the composition range included in this paper are available with the following exceptions: sulfur, millerite, brookite, cotunnite, calaverite, baddeleyite and krennerite. For the benefit of any wishing to add to the available models, the following list gives all structural types within the composition range included in this paper, for which model calculations have not yet been made:

Formula Type					
A		AB		AB_2	
A-6	In	D-3_1	calomel	C-11	$MoSi_2$
A-10	Hg	B-13	millerite	C-12	$CaSi_2$
A-11	Ga	B-14	FeAs		
A-12α	α—Mn	B-15, B-27	FeB	C-13	HgI_2
A-13	β—Mn			C-14	$MgZn_2$
A-15	β—W	B-16	GeS	C-15	$MgCu_2$
A-16	orthorhombic-S	B-19	AuCd	C-16	$CuAl_2$
A-17	black-P	B-20, B-28	FeSi	C-19	$CdCl_2$
A-18	Cl			C-21	brookite
A-19	Po	B-21	CO	C-22	Fe_2P
		B-22	K(SH)	C-23	cotunnite
		B-23	α—AgI	C-24	$HgBr_2$
		B-24	TlF	C-26	NO_2
		B-25	γ-NH_4Br	C-27	CdI_2
		B-29	SnS	C-28	$HgCl_2$
		B-30	MnZn	C-29	SrH_2
		B-31	MnP	C-31	$Zn(OH)_2$
		B-32	NaTl	C-32	AlB_2
		B-33	TlI	C-34	calaverite
				C-36	$MgNi_2$
				C-37	Co_2Si
				C-38	Cu_2Sb
				C-39	ZrW_2
				C-40	$CrSi_2$
				C-41	Fe_2W
				C-43	baddeleyite
				C-44	GeS_2
				C-46	krennerite

The Structures of the Elements

A-1, *Copper*,[10] *Fm3m* (O_h^5)

Copper illustrates the structure of several of the common face-centered cubic metals. After drilling, the first hole is not utilized, and the initial holes of all balls are pointed in the direction of the same axis. The closest interatomic distance, $d = 2.55$Å, has been altered to 2.50Å to

[10] S$_I$., pp. 13–14; W., pp. 200; B., pp. 48–50.

meet the requirements of available ball sizes. The model is assembled most easily by constructing (100) sheets and pinning them together, omitting certain of the pins between the adjacent planes.

A-2, *α-Iron*,[11] $Im3m$ (O_h^9)

α-iron illustrates the structure of the body-centered cubic metals. Although it is possible to utilize drilling coördinates in which the initial hole may be pegged, the coördinates listed give a more symmetrical model, especially if more than one cell is constructed. It is desirable to point the first holes of all balls in the model in the direction of the same a-axis. The closest interatomic distance, $d = 2.477$Å, has been represented as 2.500Å in the model. The structure is assembled by constructing (110) sheets and later fastening them together.

A-3, *Magnesium*,[12] $C6/mmc$ (D_{6h}^4)

Magnesium is a representative example of hexagonal closest packing with axial ratio $c:a = 1.625:1$. The distances between atoms, 3.20Å in the (0001) plane and 3.19 between adjacent (0001) planes, have both been changed in the model to 3.25Å. The initial holes are not used and point in the direction of the c-axis. The model is best assembled by constructing (0001) sheets and pinning them together. The structure is so tight that no weakness results if certain pins are omitted to facilitate construction.

A-4, *Diamond*,[13] $Fd3m$ (O_h^7)

Diamond illustrates the simple tetrahedral structure. The interatomic distance, 1.542Å, has been slightly changed in the model, where it is represented as 1.500Å. The model is most readily assembled by constructing (111) sheets and pinning one completed sheet to the next. The initial hole is utilized.

A-5, *White Tin*,[14] $I4/amd$ (D_{4h}^{19})

White tin has a distorted tetrahedral structure which can be considered as a diamond structure collapsed along one of the three cubic axes. The simplest cell is a body-centered one derived by a reorientation of the (100) and (010) planes of the face-centered diamond into (110) and ($\bar{1}10$) planes of white tin. The interatomic distance, 3.02Å, has been represented in the model as 3.00Å. The first hole of each ball is not used and points in the direction of the c-axis. The model is assembled most easily by pinning together separate (001) sheets.

[11] SI., pp. 15–16; W., p. 202; B., pp. 48–50.
[12] SI., pp. 16–19; W., pp. 200–201.
[13] SI., pp. 19–21; W., p. 202; B., pp. 51–53.
[14] SI., pp. 21–23; W., p. 211.

A-7, *Bismuth*,[15] $R\bar{3}m$ (D_{3d}^5)

Bismuth may be regarded as having a distorted simple cubic structure. Actually, it is composed of separate basal sheets. The closest interatomic distance, $d = 3.10$Å, is represented in the model as 3.125Å. Each atom is bonded to three close neighbors in contact at distance d and in the same basal sheet, and to two others vertically one sheet above and two sheets below by means of spacing bars whose lengths are respectively 1.97 and 2.31 inches. These bar lengths are calculated on the basis that depth of holes drilled in the balls is exactly $\frac{3}{8}$ inch. The longer spacing bar is utilized between initial holes (which point towards each other in the structure) and the shorter bar between $\rho = 180°$ holes. The bars are aligned in the direction of the principal axis of the resulting rhombohedron which is also the direction in which initial holes are pointed.

A-8, *Selenium*,[16] $C3_12$, $C3_22$ (D_3^4, D_3^6)

The closest interatomic distance between selenium atoms, $d = 2.32$Å, is adjusted to 2.375Å in the model. The structure consists of strings of selenium atoms spiralling about three-fold screw axes through the lattice points, with contact between atoms in an individual string, and with strings separated from one another at non-packing distances.

This model is conveniently made by constructing (0001) sheets of balls separated by spacing bars. The balls are translation equivalents arranged at points of a hexagonal plane lattice. The basal planes are fastened together by pinning atoms in contact so that the strings are arranged along vertical screw axes.

Spacing bars are cut 1.78 inches long for use in holes of $\frac{3}{8}''$ depth. The initial holes point in the direction of the c-axis and are not bonded.

A-9, *Graphite*,[17] $C6mc$ (C_{6v}^4)

Graphite consists of planes composed of rings of carbon atoms with individual planes separated by greater than packing distances. The interatomic distance, 1.42Å, is represented as 1.375Å. There are two kinds of carbon atoms in the structure which alternate with each other in any of the hexagonal rings composing an individual (0001) plane. The difference is indicated by the diagram in the reference: above and below one kind, C_1, lies a similar atom, C_1, in adjacent planes at $\pm c/2$ distance; whereas the other kind, C_2, lies in planes at $\pm c/2$ above and below the open center of a hexagonal ring. Two separate drillings are required, one for C_1, the other for C_2. All initial holes point in the direction of the

[15] S$_I$., pp. 25–27; W., pp. 202–203; B., pp. 50–51.
[16] S$_I$., pp. 27–28; W., p. 203.
[17] S$_I$., pp. 28–30; W., p. 208; B., pp. 52–54.

c-axis. Spacing bars 1.51 inches long hold the (0001) planes apart at distance $c/2$. All holes are $\frac{1}{4}''$ deep and tie pins are $\frac{3}{8}''$ long.

A-14, *Iodine*,[18] *Ccma* (D_{2h}^{18})

The closest interatomic distance between iodine atoms, 2.70Å, is represented in the model as 2.75Å. The entire structure is proportionally enlarged in the model. Revised cell constants are:

$a=4.9$Å
$b=7.4$Å
$c=9.95$Å

As each atom is in close packing contact with but one neighbor, the model must be constructed on a wooden baseboard representing the (010) plane as shown in figure 1. Holes are drilled in the baseboard at the indicated positions. Long brass rods are inserted in these holes, and paired atoms are suspended on the brass rods. After the usual drilling of the balls, the initial hole is redrilled completely through the ball.

The centers of the pairs along the same set of pins are spaced at intervals corresponding to the unit length on b, 3.7 inches. Pairs along adjacent sets of pins are spaced similarly but their centers are located at $b/2$ positions.

A-17, *Black Phosphorus*,[19] *Bmab* (D_{2h}^{18})

Black phosphorus has a layer structure. Each phosphorus atom is in packing contact with three other atoms in its own layer and equidistant from two others on the same symmetry plane in a neighboring layer. The layers are physically supported in the model with the aid of space bars 1.612 inches long, extending in the last-mentioned directions.

In the actual structure the distances between phosphorus atoms in the same layer are 2.17Å and 2.20Å. In the model, the parameter has been changed from .090 to .0863 to equalize all interatomic distances between immediate neighbors in the same layer to 2.19Å. This distance has been represented in the model as 2.25Å, and all dimensions of the model scaled up in this same ratio.

Structures of the AB Type

B-1, *Halite*,[20] *Fm3m* (O_h^5)

Halite can be very closely represented by altering the Na-Cl interatomic distance, $d=2.814$Å, so that the scale distance in the model is 2.8125Å. The structure is readily assembled by constructing (100) planes and pinning them together. It is best to have the initial holes of all balls pointing in the direction of the same a-axis.

[18] W., pp. 209–210; S$_{II}$ p. 5.

[19] S$_{III}$., p. 6.

[20] S$_{I}$., pp. 72–74; W., p. 215; B., pp. 57–60.

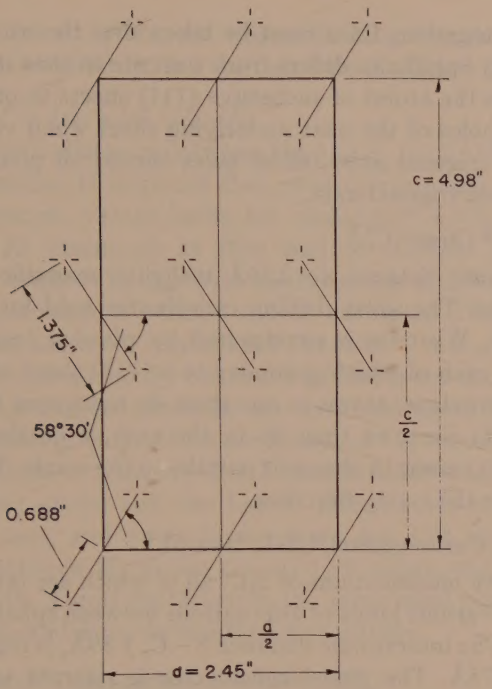

FIG. 1. Layout of baseboard for the construction of the iodine model. The edges of the board are not shown. The heavy rectangle outlines the unit cell and the crosses locate the positions for holes into which supporting rods are to be set.

B-2, *Caesium Chloride*,[21] $Pm3m$ (O_h^1)

Caesium chloride, although not occurring in nature, is an important representative of a type of AB structures which includes several alloys. The model is a scale representation of the structure in that there is no change in the interatomic distances. The initial holes are not used and point in the direction of one of the axes. A model of more than one cell can be constructed most readily by fastening together adjacent (110) planes as in alpha-iron.

B-3, *Sphalerite*,[22] $F\bar{4}3m$ (T_d^2)

Sphalerite is a simple tetrahedral array of alternating zinc and sulphur atoms based on the diamond pattern. The interatomic distance, $d=2.35$Å, is represented in the structure as 2.375Å. The model is most readily assembled by first constructing (111) sheets, which are composed of puckered hexagonal rings of alternating zinc and sulphur, and then

[21] S$_{I.}$, pp. 74–77; W., p. 214.

[22] S$_{I.}$, pp. 76–77; W., pp. 215–216; B., pp. 62–65.

pinning these together. Care must be taken that the wurtzite structure does not result. Sphalerite differs from wurtzite in that its face-centered lattice requires the atoms of successive (111) sheets to occupy positions screening the holes of the next underlying sheet when viewed from the direction of a trigonal axis. Initial holes should all point in the direction of the same trigonal axis.

B-4, *Wurtzite*,[23] *C6mc* (C_{6v}^4)

The interatomic distance, $d = 2.36$Å, is slightly magnified in this model, as in sphalerite. The same drilling coördinates hold for both wurtzite and sphalerite. Wurtzite is constructed by pinning together adjacent (0001) sheets, each of which is similar to a (111) sheet of sphalerite. In the wurtzite structure, atoms in one sheet do *not* screen the holes in the adjacent (0001) sheet as they do in the case of octahedral sheets in sphalerite. This results in channels parallel to the *c*-axis. The initial holes should point in the *c*-axis direction.

B-5, B-6, B-7, *Carborundum*,[24] III, II, and I

There are five modifications of SiC, all of which are tetrahedral structures showing various kinds of alternations between sphalerite and wurtzite packing. The interatomic distance $S-C$, 1.89Å, is represented in the models as 1.875Å. The model constructor is referred to the *Strukturbericht* reference for details of stacking sequence (especially S_I p. 84) and for decision as to the appropriate number of balls necessary to give a representative picture of the unit cell.

B-8, *Niccolite*,[25] *C6mc* (C_{6v}^4)

The closest packing distance between Ni and As atoms, 2.43Å, is represented as 2.4375Å. The Ni-Ni interatomic distance, 2.52Å, is represented as 2.50Å. Nickel atoms lie in packing contact with each other along columns in the *c*-axis direction. Initial holes of all balls should point in the *c*-axis direction.

B-8, *Pyrrhotite*,[26] *C6mc* (C_{6v}^4)

The arrangement of atoms in pyrrhotite is similar to that in niccolite, but the cell is more expanded in the direction of the *c*-axis. As a result of this, the metals do not touch, as they do in the niccolite structure. The metal atoms have a perfectly regular octahedral sulfur coördination. The Fe—S distance is actually 2.47Å in the structure; it is represented as 2.50Å in the model, and all dimensions are expanded by this amount.

[23] S_I., pp. 78–79; W., pp. 216–217; B., pp. 64–65.
[24] S_I., pp. 80–84; W., pp. 222–223.
[25] S_I., pp. 84–87; W., p. 217; B., pp. 65–68.
[26] S_I., pp. 84–87; W., pp. 217–218; B., pp. 65–68.

In calculating this structure, the original drilling coördinates have been transformed by rotation so that the first hole is utilized for bonding.

B-9, *Cinnabar*,[27] $C3_12$, $C3_22$ (D_3^4, D_3^6)

The interatomic distance between Hg and S, $d=2.52$Å, is altered to 2.50Å in the model. It is stated that uncertainty exists as to which of the two parametric values holds for cinnabar:[28] $u=0.33$, $v=0.21$ or $u=0.72$, $v=0.55$. Inasmuch as they lead to different structures, the coördinates for both are listed. With the exception of different drilling coordinates, generalizations pertain to both examples. The lengths of the a-axis and c-axis are truly represented (Buckley's values).

The model is assembled by constructing sheets consisting of Hg balls at points of a hexagonal plane lattice and held apart at non-packing distances by spacing bars. Alternate sheets of Hg atoms are united by intermediate layers of S atoms; each S atom is bonded to two Hg atoms, one in the sheet above and one below. Initial holes of both types of balls are not used, and point in the same direction along the c-axis. Spacing bars between Hg atoms are cut 1.39 inches long, for seating in holes $\frac{3}{8}''$ in depth. Atoms contained in the same basal plane are translation equivalents and must be oriented accordingly.

B-11 *Lead Oxide*,[29] (tetragonal), $P4/nmm$ (D_{4h}^7)

This is a layer structure composed of identical (001) sheets held together by space bars. The interatomic distance between Pb and O, 2.33Å, is represented in the model by a scale distance of 2.3125Å. An imperceptible contraction of the a-axis occurs in the model but, as spacing bars are used between (001) sheets, their lengths are adjusted so that c is truly represented. Initial holes in Pb are utilized for spacing bars and point in the direction of the tetragonal axis. Easiest assembly is by constructing 100 strings of Pb-O-Pb-O-Pb, etc., attaching these to form (001) sheets, and then fastening the sheets together with space bars $1\frac{5}{8}''$ long.

D-31, *Calomel*,[30] I $4/mmm$ (D_{4h}^{17})

Ball sizes have been chosen on the assumption that the opposing chlorine atoms of neighboring layers are in contact. The Hg-Cl interatomic distance, 2.52Å is represented in the model as 2.50Å. The entire structure is correspondingly shrunk by less than 1%. The c-axis, in addition, loses .1Å by the ball sizes chosen, but this can be compensated,

[27] Sr., pp. 87–89; W., pp. 221–222; B., pp. 68–69.
[28] W., p. 222.
[29] Sr., pp. 89–95; W., pp. 218–219.
[30] Sr., pp. 237–239.

if desired, by the use of a spacing bar of .80″ length between opposing chlorines ($\rho = 0°$) set in holes $\frac{3}{8}$″ deep.

B-12, *Boron nitride*,[31] *C6mc* (C_{6v}^4)

The boron nitride structure is the same as the graphite structure in which B takes the place of C_2 and N takes the place of C_1, The interatomic packing distance in the (0001) sheets, $d = 1.45$Å, is represented in the models by 1.4475Å. Spacing bars are 1.48 inches long and hold the (0001) planes apart at distance $c/2$. All holes are $\frac{1}{4}$″ deep and tie pins are $\frac{3}{8}$″ long.

B-18, *Covellite*,[32] *C6/mmc* (D_{6h}^4)

The covellite structure consists of hexagonal basal sheets, each composed of copper and sulfur atoms. There are two kinds of copper atoms and two kinds of sulfur, each restricted to a unique type of coördination within the structure. Starting with a sheet composed of S_{II} and Cu_{II} (see Fig. 2), the next sheet is a true plane of S_I and Cu_I in alternating

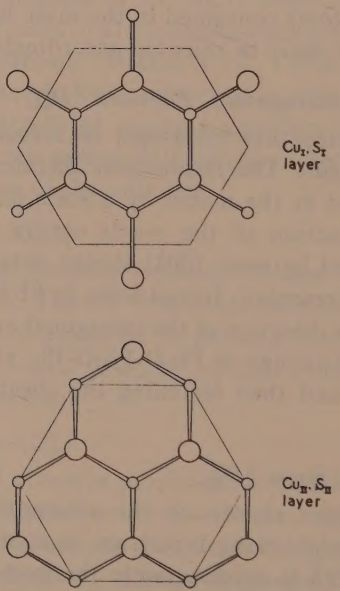

FIG. 2. Plans of the two different kinds of (0001) layers in the covellite structure, showing bonding within the layers. The hexagon drawn in fine lines outlines the hexagonal cell (containing three primitive translation units). The large circles represent Cu atoms, the small circles, S atoms.

[31] S$_{I}$., p. 95; W., p. 208.
[32] S$_{II}$., pp. 10–11; B , p. 77.

hexagonal array and at level c 4. There is a reflection plane of symmetry contained in all planes composed of Cu_I and S_I, so the next sheet is a duplicate of the first. This completes half the cell. A duplicate sequence is next constructed, rotated 180° from the first, and attached to it, bonding S_{II} of the lower unit to S_{II} to the upper one. All initial holes point in the c-axis direction.

The following tabulation indicates the liberties which have been taken with the actual structure.

	Structure	Model
Cell constants: a	3.80Å	3.77Å
c	16.46Å	16.50Å
Interatomic distances		
S_{II}-S_{II}	2.05Å	2.00Å
S_{II}-Cu_{II}	2.32Å	2.3125Å
S_I-Cu_I	2.20Å	2.1875Å
Cu_{II}-S_I	2.34Å	2.375Å

It is possible to adjust the structure in other directions, but the adjustments outlined above cause little deviation from the actual structure. The bond angles for S_I and Cu_I, 109°, are very close to the tetrahedral angle, 109° 28′.

B-17, *Cooperite*,[33] $P4/mmc$ (D^9_{4h})

The interatomic distance between Pt and S atoms, 2.32Å, is represented in the model as 2.3125Å. Initial holes of Pt are not used and point in the same [100] direction within any (001) plane; initial holes of Pt in the adjacent planes point in the [010] direction. Initial holes of S point in the [001] direction and are not bonded. Easiest assembly is accomplished by pinning together separate (011) planes. A primitive cell gives a very poor representation of the structure; it is best to construct a C-centered one, which, incidentally, is then directly comparable with the tenorite structure.

B-26, *Tenorite*,[34] $C2/c$ (C^6_{2h})

This is a slightly collapsed cooperite structure. In order to construct it, it is highly desirable to have a C-centered cooperite structure already made, as a guide. Figure 1 of Tunell, Posnjak and Ksanda's article[35] should first be altered as follows: draw colored lines between Cu and O atoms to show approximately square Cu bonds and approximately tetrahedral O bonds. Then label all oxygens on the $\frac{c}{4}$ level "L" (left) and all those on the $\frac{3c}{4}$ level "R" (right).

[33] S_{II}, pp. 9–10; B., pp. 69–70.
[34] B., pp. 92–93; S_{III}, pp. 11–12.
[35] *Zeits. Krist.*, (A) vol. 90, p. 134, 1935.

The mark between holes in the oxygens gives the direction of the 2-fold axis on which these lie, and fixes the orientation. The mark between holes in the coppers identifies the acute angle of the almost square bonds. This acute bisector should lie in the (001) plane.

The assembly in this model is best made (if the model is one cell plus environs as included in the table) by constructing the lower [101] ribbons of the type

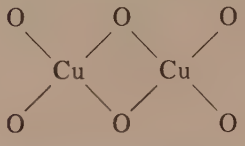

and adding crossing [10$\bar{1}$] ribbons thereto. For larger models, the cooperite type of construction should be followed, i.e., by fitting together (111) sheets. This construction method is exceedingly difficult because of the many orientation requirements involved.

Structures of the AB_2 Type

Many of these structures are closely represented by the models on the scale adopted. Those in which the atoms lie in special positions have had ball sizes so chosen as to represent most closely the interatomic distances. The departures from true representation are therefore but slight magnifications or contractions of interatomic distance and cell edges.

More serious distortions have to be compensated in structure where the atoms lie in positions with variable parameters as in the case of marcasite. In general, these difficulties are overcome as in marcasite by the method discussed in the earlier paper.[1]

Special problems for successful construction of models are presented by the silica minerals; the final section of this paper will illustrate the type of adjustment utilized in calculating the drilling coördinates for these structures.

C-1, *Fluorite*,[36] *Fm3m* (O_h^5)

The interatomic distance between Ca and F, $d = 2.362$Å, is represented in the model as 2.375Å. Initial holes are not used, and point in the direction of the same cubic axis. Notwithstanding the simplicity of the structure, the model is difficult to construct because of its exceedingly close packing. If more than a unit cell is built, it is easiest to construct separate (110) planes and pin them together, omitting all but necessary pins.

[36] S$_{I.}$, pp. 148–150; W., p. 230; B., p. 57.

C-2, *Pyrite*,[37] *Pa*3 (T_h^6)

The interatomic distance between S atoms, $d = 2.10$Å, is represented in the model as 2.125Å. The Fe-S distance, $e = 2.26$Å, is represented as 2.25Å. The cell edge in the model is represented as 5.38Å as compared with 5.40Å in the actual structure.

This structure is so complex that it is necessary to understand the space group before attempting construction. Initial holes of balls representing Fe atoms are not used and must point in the direction of a 3-fold axis in the space group. The initial hole of S is everywhere bonded to the initial hole of the other S constituting the sulfur pair. Easiest construction is realized by pinning together individual strings made up of Fe-S-S-Fe or S-S-Fe-S-S which are elongated in the direction of a cubic axis. The strings are then joined to form (100) sheets, which are subsequently pinned together.

C-3, *Cuprite*,[38] *Pn*3*m* (O_h^4)

The cuprite structure consists of two identical space networks which thread through one another's interstices but in no place come in contact. Because of this unusual situation, in the model representation of the structure one network must be suspended from the other by space bars of arbitrary location. The individual networks have an arrangement identical with that of cristobalite in which the cristobalite silicon has been replaced by the cuprite oxygen and the cristobalite oxygen has been replaced by the cuprite copper.

The closest interatomic distance between Cu and O, $d = 1.84$Å, is represented in the model as 1.875Å. Spacing bars 1.67 inches long extend vertically from the O of one network to the O of the other. Holes in O are drilled $\frac{3}{8}''$ deep, in Cu $\frac{1}{4}''$. Tie pins must be $\frac{1}{2}''$ long instead of the usual $\frac{5}{8}''$ length. The spacing bars are all located in the direction of the vertical axis. The model is constructed by pinning together, *via* the Cu balls, separate (110) planes containing both Cu and O.

C-4, *Rutile*,[39] *P*4/*mnm* (D_{4h}^{14})

Interatomic distances, $d = 2.01$Å, between Ti and O, and $e = 2.46$Å, between O and O, are represented in the model by 2.00Å and 2.50Å, respectively. The model is most easily constructed by assembling separate (110) planes.

C-5, *Anatase*,[40] I4/*amd* (D_{4h}^{19})

The interatomic distances in the anatase structure have been ad-

[37] St., pp. 150–153; W., p. 234; B., pp. 71–73.
[38] St., pp. 153–155; W., p. 241; B., pp. 90–91.
[39] St., pp. 155–158; W., pp. 230–231; B., pp. 102–103.
[40] St., pp. 158–161; W., pp. 249–250; B., p. 104.

justed in the model in order to correspond with the ball sizes adopted for rutile. The model is constructed by assembling (001) sheets of Ti and O balls. The initial holes of all balls point in the c-axis direction. The alterations are as follows:

	Structure	Model
(*d*) Ti-O	1.95Å	2.00
(*d'*) Ti-O	1.91Å	2.00
(*e'*) O-O	2.43Å	2.50

C-6, *Tin Disulphide*,[41] *C3m* (D_{3d}^3)

Tin disulphide has been taken as a convenient representative of the "cadmium iodide structure." It can be represented either as an ionic bond structure or as a covalent bond structure, data for both being given in the tables. The Sn–S distances are 2.55Å in the actual structure; they are represented as 2.50Å in the models. The closest S–S distances are 3.59Å and 3.62Å in the actual structure; they are all idealized to 3.562Å in the models.

If ionic bonding is assumed, the structure can be represented by hexagonal close-packed S ions in contact (construction the same as the magnesium model) with Sn ions stuffed into the interstices between sulfur octahedra. For this model, a single hole is drilled in the Sn ion to attach it to one of its six neighboring sulfur ions.

If covalent bonding is assumed, the structure becomes a series of identical, separated sheets. The sheets are kept together by means of space bars, 2.175 inches long and parallel to the *c* axis, extending between tin atoms.

C-7, *Molybdenite*,[42] *C6/mmc* (D_{6h}^4)

This is a layer structure, composed of separate hexagonal MoS_2 layers. The layers are separated from one another at greater than packing distances, arranged for in the model by means of spacing bars. The interatomic distance, $d = 2.35$Å, is altered to 2.375Å in the structure. The lengths of the *a*-axis and *c*-axis in the model truly represent the structural axes. All initial holes point in the direction of the *c*-axis but it is not necessary to place a spacing bar in every position available. Spacing bars are cut 1.87″ long for holes $\frac{3}{8}$″ in depth.

C-18, *Marcasite*,[43] *Pnnm* (D_{2h}^{12})

The adjustment of the marcasite structure has been discussed in the earlier paper.[44] Several other compounds, löllingite, FeP_2, $FeSb_2$, and

[41] S$_{I}$., pp. 161–163; W., pp. 232–233.
[42] S$_{I}$., pp. 164–166; W., p. 233; B., p. 77.
[43] S$_{I}$., pp. 495–497; S$_{II}$., p. 272; WS., pp. 23–26; B., pp. 73–75.
[44] Reference 1, pp. 160–167.

$CaCl_2$, whose structures are of the marcasite-type have been adjusted and calculated in a similar manner. Their coördinates are listed without comment.

In structures where balls are drilled with holes at nearly equal ρ angles as in marcasite, it is well to mark certain holes with a scratch or prick of the drill bit on the ball surface in order to facilitate identification of this hole and thus easy orientation when assembling. Holes thus marked are noted with an "m" in the tabulation.

C-18, *Löllingite*,[45] *Pnnm* (D_{2h}^{12})
See under *marcasite*, above.

C-18, *Iron di-phosphide*,[46] *Pnnm* (D_{2h}^{12})
See under *marcasite*, above.

C-18, *Iron di-antimonide*,[47] *Pnnm* (D_{2h}^{12})
See under *marcasite*, above.

C-18 (C-35), *Hydrophilite*,[48] *Pnnm* (D_{2h}^{12})
See under *marcasite*, above. Hydrophilite has a marcasite-like structure, but the Cl atoms are not so obviously paired.

C-42, *Silicon di-sulfide*,[49] *Icma* (D_{2h}^{26})

The structure consists of individual strings of SiS_2 along sets of B-centered *b*-axes. A wooden baseboard has a rectangle laid off on it to represent the unit cell in the (010) plane, $a = 2.8$ inches and $c = 4.8$ inches. At the corners and the center of this rectangle, holes are drilled and long brass rods inserted into them. The balls representing Si have their initial holes drilled all the way through and these are impaled on the rods and held apart by balls representing S. The strings are of two configurations, right and left.

To construct a single cell, make four strings as follows:

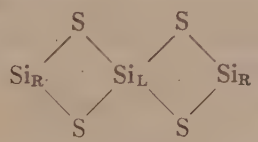

and place these at the cell corners. Make up one string as follows:

[45] S_{II}, pp. 273–274; B., pp. 73–75; WS, pp. 23–26.
[46] WS, p. 24; S_{III}., p. 310.
[47] S_I., p. 497.
[48] S_{III}., pp. 30–31, p. 278.
[49] S_{III}., pp. 37–38, 286.

and place it at the cell center.

C-9, *High Cristobalite*[50] (Ideal, after Wyckoff), $Fd3m$ (O_h^7)

The interatomic O–O distance, $d = 2.52$Å, is adjusted to 2.50Å. Silicon ions are represented by small glass beads or lead pellets. They are not pinned, for the size chosen fits exactly into the interstitial space within the four oxygen members of a tetrahedron. Buckshot, 0.30″ in diameter are satisfactory (No. 1 Buckshot, eastern size; no. 5 or 6 buckshot, western size).

The model is most readily assembled by constructing individual rows of tetrahedra in the [110] direction and pinning them together. The initial holes point towards the unpinned Si pellet.

C-30, *Low Cristobalite*,[51] $P4_12_1$, $P4_32_1$ (D_4^4,D_4^8)

The adjustment of the low cristobalite structure for the derivation of drilling coördinates of the model is given in the appendix. Several of the silica structures have undergone somewhat similar adjustments. The principal adjustment of the actual structures is an idealization of slightly distorted SiO_4 tetrahedra. The actual O–O distances, which vary from 2.58–2.63Å, are represented in the model as 2.625Å.

The initial hole of O is not used, and points in the direction of the c-axis. The model is most easily constructed by assembling individual tetrahedra, pinning them into rows, and uniting the rows.

C-10, *High Tridymite*,[52] $C6/mmc$ (D_{6h}^4)

The interatomic O–O distance, 2.52Å, is represented in the model as 2.50Å. The structure is composed of hexagonal rings of O_I atoms in the (0001) plane, united to the adjacent (0001) plane by O_{II} atoms which are mutually shared by upper and lower tetrahedra. The initial holes of O_I point towards a Si but are not used, and the unused initial holes of O_{II} point towards Si, which direction is also the c-axis direction. The model is assembled by uniting (0001) planes.

C-8, *High Quartz*,[53] $C6_22$, $C6_42$ (D_6^4, D_6^5)

The interatomic O–O distance, 2.59Å, is represented in the model as 2.625Å. Initial holes are not used and point towards an unbonded Si

[50] S$_I$., pp. 169–171; B., pp. 88–90; WS., pp. 28–29.
[51] S$_{III}$, pp. 25–26.
[52] S$_I$., pp. 171–174; B., p. 88; W., pp. 248-249.
[53] S$_I$., pp. 166–169; W., pp. 246-247; B., pp. 84–85.

pellet. The model is best assembled by assembling separate (0001) planes of tetrahedra.

"C-8," *Low Quartz*,[54] $C3_12$, $C3_22$, (D_3^4, D_3^6)

Although each oxygen atom actually has four different coördination distances to other oxygens varying from 2.62Å–2.57Å, the structure has been idealized by representing all O-O spacings as 2.625Å. Initial holes are not used and point in the *c*-axis direction. The model is best assembled by constructing individual rows of tetrahedra, and uniting to form (0001) planes. The adjustment of this structure to drilling coördinates was made in a similar way to that of low cristobalite described in the appendix.

Appendix

Coordinate Calculations in Cases of Low Bond Symmetry.

General Procedure.—Many of the structures which have been discussed have been characterized by atoms situated in positions of considerable symmetry. In such cases the distribution of nearest neighbors and, therefore, the distribution of mechanical bonds in the model have been symmetrical. In structures containing atoms in positions of little or no symmetry, the methods of calculating drilling coördinates which have been discussed are ordinarily ones of very great difficulty. The more general cases are readily treated by the following simple general principles:

The necessary adjustments are first accomplished and new coördinates of the atoms calculated for the adjusted structure. If the crystal is not isometric, *these coördinates must be transformed into new ones referred to isometric, orthogonal axes*. This is ordinarily easily accomplished except for triclinic crystals, where the transformation is tedious. An example of the transformation for monoclinic crystals is given beyond. Let the new coördinates of two atoms be $[[x_1y_1z_1]]$ and $[[x_2y_2z_2]]$. The drilling coördinates of the bond from atom 1 to atom 2, referred to the new Z axis as origin direction, can be seen from figure 3 to be:

$$\rho = 90° - \tan^{-1}\left(\frac{z_2 - z_1}{\sqrt{(x_2-x_1)^2+(y_2-y_1)^2}}\right) \tag{1}$$

or

$$\rho = 90° - \sin^{-1}\left(\frac{z_2 - z_1}{\sqrt{(x_2-x_1)^2+(y_2-y_1)^2+(z_2-z_1)^2}}\right) \tag{2}$$

where $\sqrt{(x_2-x_1)^2+(y_2-y_1)^2+(z_2-z_1)^2}$ is the interatomic distance.

$$\phi = \tan^{-1}\left(\frac{y_2-y_1}{x_2-x_1}\right). \tag{3}$$

[54] WS., p. 26; B., p. 85; S_{III}, p. 21.

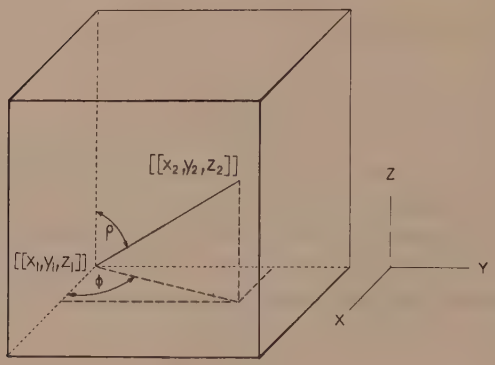

FIG. 3. The derivation of the drilling coördinates, ρ and ϕ, for a bond extending from a ball with coördinates $[[x_1, y_1, z_1]]$, to a ball with coördinates $[[x_2, y_2, z_2]]$. The origin direction for drilling coördinate ρ is Z.

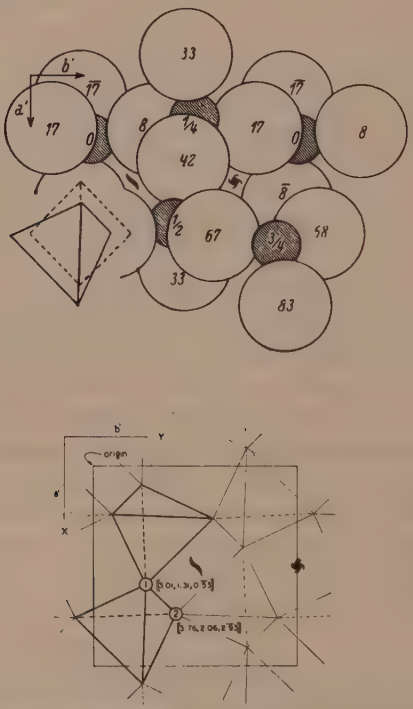

FIG. 4A. Nieuwenkamp's illustration of the structure of low cristobalite projected on (00$\bar{1}$).

FIG. 4B. Diagrammatic representation of the adjusted low cristobalite structure corresponding with part of Fig. 4*A*, and illustrating the derivation of the drilling coördinates for the bond extending from oxygen atom 1 to oxygen atom 2.

The origin direction, Z, which becomes the first, unused, hole, may be any of the coördinate directions which it is convenient to use. The only restriction on the choice of the direction, Z, is that it should not have a bond nearer to it than about $\rho = 30°$, for such holes are mechanically impossible to drill.

Application to low-cristobalite drilling coördinates.—The low-cristobalite structure[55] furnishes an illustration of the usefulness of this general method. The bonds are between oxygen atoms occupying the general position of a structure of low symmetry. Low cristobalite is tetragonal $P4_12_1(D_4^4)$ and has a structure projected on (001) as shown in Fig. 4*A*.

The adjustments need not be discussed in detail. They include regularizing the slightly irregular SiO_4 tetrahedron and shrinking the actual cell dimensions slightly to permit the use of commercial ball sizes. The new coördinates of two atoms, referred to an isometric coördinate system are shown in Fig. 4*B*. Utilizing the relations given above, the drilling coördinates of the bond from atom (1) to atom (2) are:

$$\rho = 90° - \tan^{-1}\left(\frac{\overline{2.03} - \overline{.53}}{\sqrt{(3.76-3.01)^2+(2.06-1.31)^2}}\right)$$
$$= 90° - (-66°) = 156°$$
$$\phi = \tan^{-1}\left(\frac{(2.06-1.31)}{(3.76-3.01)}\right)$$
$$= 45°.$$

Application to tenorite drilling coördinates.—A simple example in which generalized crystal coördinates must first be transformed into isometric orthogonal coördinates, is afforded by the structure of tenorite.[56] Tenorite is monoclinic, and has a structure which can be described as a somewhat collapsed cooperite structure. Each copper atom is surrounded by four oxygen atoms at the corners of an almost square rectangle, and each oxygen atom is surrounded by four copper atoms at corners of an irregular tetrahedron of symmetry C_2. The collapse and consequent irregularity of the coördinations give rise to the monoclinic nature of the structure.

All Cu-O distances between immediate neighbors are given by the investigators as 1.95Å. This can be represented in commercially available ball sizes by 1.9375Å (1 15/16″). Since no adjustments except the change of scale are required, the structure of tenorite can be exactly represented in a model by allowing an all-around linear shrinkage of about $\frac{1}{2}\%$.

[55] Nieuwenkamp, W., Die Kristallstruktur des Tief-Cristobalits SiO_2. *Zeits. Krist.*, Vol. **92**, pp. 82–88, 1935.

[56] Tunell, G., Posnjak, E., and Ksanda, C. J., Geometrical and optical properties, and crystal structure of tenorite: *Zeits. Krist.*, vol. **90**, pp. 120–142, 1935.

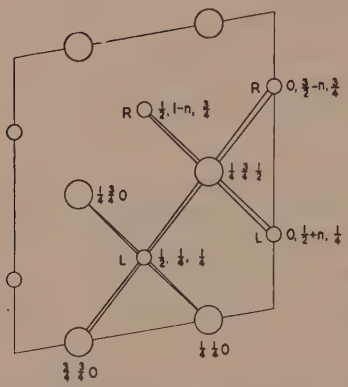

FIG. 5A. Projection of the structure of tenorite on $(0\bar{1}0)$, showing the bonding between atoms having the coördinates indicated. Large circles are copper atom positions, small circles are oxygen atom positions. The designations "L" and "R" indicate atoms whose environments and drilling coördinates are related to one another as left and right, respectively. The fine lines outline the unit cell.

FIG. 5B. The derivation of isometric orthogonal coördinates, X, Y, and Z from the monoclinic coördinates, x, y, and z. The direction Y is to become the origin direction for drilling coördinates ρ.

Figure 5*A* shows a duplicate of Tunell, Posnjak and Ksanda's Fig. 2*c*, which is a projection of tenorite on $(0\bar{1}0)$, but slightly modified to bring out the bonding. The relation between the monoclinic coördinates and isometric coördinates taken parallel and perpendicular to the monoclinic *c*-axis, is shown in Fig. 5*B*. The new isometric coördinates, XYZ, are evidently derivable from the monoclinic coördinates xyz with the aid of the following transformation:

$$X = ax \cos(\beta - 90)$$
$$Y = b\,y$$
$$Z = c\,z - ax \sin(\beta - 90)$$

Carrying out these transformations for the eight atoms linked by bonds as in Fig. 5*A*, yields the isometric orthogonal coördinates listed in Table I.

The drilling coördinates may now be calculated by substituting the isometric orthogonal coördinates in relations like (1) and (3) but such as to make $\overline{Y}$ the origin of ρ. For example, in calculating the drilling coördinates for the copper at $[[\frac{1}{4}\ \frac{3}{4}\ \frac{1}{2}]]$, the coördinates for the hole to the oxygen at $[[0,3/2-n,\frac{3}{4}]]$ are,

$$\rho = 90° - \tan^{-1}\left(\frac{3.831-2.362}{\sqrt{(0-1.147)^2+(3.124-2.558)^2}}\right)$$
$$= 90° - 48.9°$$
$$= 41.1°$$

$$\phi = \tan^{-1}\left(\frac{3.124-2.558}{0-1.147}\right)$$
$$= -26.2° = +333.8°.$$

A full calculation of the drilling coördinates to either the oxygen at $[[0,\frac{1}{2}+n,\frac{1}{4}]]$ or the oxygen at $[[\frac{1}{2},1-n,\frac{3}{4}]]$, is also needed. All other drilling coördinates may be obtained by symmetry from these two sets of coördinates because the copper is located on an inversion center and the oxygen on a two-fold rotation axis normal to the plane of the projection. Note that the symmetry of the location of the oxygens requires both *right* and *left* oxygens to be drilled.

It is desirable to transform the drilling coördinates once more so that holes of low ρ reading are avoided. For this purpose, the copper and oxygen coördinates are separately plotted on a rotating stereographic net, and the points rotated until the copper coördination rectangle is normal to the first hole (giving the bond holes all ρ coördinates of 90°) and until the first hole of the oxygen is one of the bond holes (giving the other bond holes ρ coördinates in roughly the same region). The resulting drilling data are found in the tabulation.

TABLE 1

Monoclinic and isometric orthogonal coördinates of tenorite. Atoms are listed in counter-clockwise rotary order (as seen in Fig. 5*A*) about central atoms of other species, namely Cu about *O* at $[[\frac{1}{2}\ n\frac{1}{4}]]$, and *O* about Cu at $[[\frac{1}{4}\ \frac{3}{4}\ \frac{1}{2}]]$.

Atom	Monoclinic coördinates			Isometric orthogonal coördinates (Ångstrom units)		
	x	y	z	X	Y	Z
Cu	$\frac{1}{4}$	$\frac{1}{4}$	0	1.147	0.853	−0.192
Cu	$\frac{1}{4}$	$\frac{3}{4}$	$\frac{1}{2}$	1.147	2.558	2.362
Cu	$\frac{3}{4}$	$\frac{1}{4}$	$\frac{1}{2}$	3.441	0.853	1.978
Cu	$\frac{3}{4}$	$\frac{3}{4}$	0	3.441	2.558	−0.576
O	$\frac{1}{2}$	n	$\frac{1}{4}$	2.294	1.991	0.893
O	0	$\frac{1}{2}+n$	$\frac{1}{4}$	0	3.695	1.277
O	0	$\frac{3}{2}-n$	$\frac{3}{4}$	0	3.124	3.831
O	$\frac{1}{2}$	$1-n$	$\frac{3}{4}$	2.294	5.401	3.447

$a = 4.653$ $\beta = 99°29'$
$b = 3.410$ $n = .584$
$c = 5.108$

A technique for the construction of models illustrating the arrangement and packing of atoms in crystals. M. J. Buerger and R. D. Butler. *The American Mineralogist*, vol. **21**, pp. 150–172, 1936.

Errata: p. 161, lines 5 and 6

$u_b = .203 \pm .01$

$v_c = .375 \pm .01$

p. 165, line 6

$$AH = \sqrt{\left(\frac{a}{2} - 0\right)^2 + \left(\left[\frac{b}{2} - y_b\right] - y_b\right)^2 + \left(\left[\frac{c}{2} + z_c\right] - z_c\right)^2} = 3.16 \text{ Å}.$$

p. 167, Table 1, second last line in column:

$270° - \angle ADm = 229°$

p. 168, line 14,

$V:S = 2.186$ Å

A-1, *Copper*

Atom	Ball Size	Number of balls required for one unit cell model	Drilling Coördinates		Bonded to	Key coördinate of neighboring atom
			ρ	ϕ		
Cu	$1\frac{1}{4}''$	14	0	0	unused	
			45	0	Cu	$\rho = 135$
			45	90	Cu	
			45	180	Cu	
			45	270	Cu	
			90	45	Cu	$\rho = 90$
			90	135	Cu	
			90	225	Cu	
			90	315	Cu	
			135	0	Cu	$\rho = 45$
			135	90	Cu	
			135	180	Cu	
			135	270	Cu	

A-2, *α-Iron*

Atom	Ball Size	Number of balls required for one unit cell model	Drilling Coördinates		Bonded to	Key coördinate of neighboring atom
			ρ	ϕ		
Fe	$1\frac{1}{4}''$	9	0	0	unused	
			55	0	Fe	$\rho=125$
			55	90	Fe	
			55	180	Fe	
			55	270	Fe	
			125	0	Fe	$\rho=55$
			125	90	Fe	
			125	180	Fe	
			125	270	Fe	

A-3, *Magnesium*

Atom	Ball Size	Number of balls required for one unit cell model	Drilling Coördinates		Bonded to	Key coördinate of neighboring atom
			ρ	ϕ		
Mg	$1\frac{5}{8}''$	17 hex	0	0	unused	
			35	0	Mg	$\rho=145$
			35	120	Mg	
			35	240	Mg	
			90	30	Mg	$\rho=90$
			90	90	Mg	
			90	150	Mg	
			90	210	Mg	
			90	270	Mg	
			90	330	Mg	
			145	0	Mg	$\rho=35$
			145	120	Mg	
			145	240	Mg	

A-4, *Diamond*

Atom	Ball Size	Number of balls required for one unit cell model	Drilling Coördinates		Bonded to	Key coördinate of neighboring atom
			ρ	ϕ		
C	$\frac{3}{4}''$	26	0	0	C	$\rho=0$
			$109\frac{1}{2}$	0	C	$\rho=109\frac{1}{2}$
			$109\frac{1}{2}$	120	C	
			$109\frac{1}{2}$	240	C	

A-5, *White Tin*

Atom	Ball Size	Number of balls required for one unit cell model	Drilling Coördinates		Bonded to	Key coördinate of neighboring atom
			ρ	ϕ		
Sn	$1\frac{1}{2}''$	13 P	0	0	unused	
		26 F	75	0	Sn	$\rho=75$
			75	180	Sn	
			115	90	Sn	$\rho=115$
			115	270	Sn	

A-7, *Bismuth*

Atom	Ball Size	Number of balls required for one unit cell model	Drilling Coördinates		Bonded to	Key coördinate of neighboring atom
			ρ	ϕ		
Bi	$1\frac{9}{16}''$	27	0	0	2.31″ spacing bar to Bi	$\rho=0$
			180	0	1.97″ spacing bar to Bi	$\rho=180$
			122	0	Bi	$\rho=122$
			122	120	Bi	
			122	240	Bi	

A-8, *Selenium*

Atom	Ball Size	Number of balls required for one unit cell model	Drilling Coördinates		Bonded to	Key coördinate of neighboring atom
			ρ	ϕ		
Se	$1\frac{3}{16}''$	16 28 hex	0	0	unused	
			45	90	Se	$\rho=135$
			90	0	spacing bar	$\rho=90$
			90	60	spacing bar	
			90	120	spacing bar	
			90	180	spacing bar	
			90	240	spacing bar	
			90	300	spacing bar	
			135	30	Se	$\rho=45$

A-9, *Graphite*

Atom	Ball Size	Number of balls required for one unit cell model	Drilling Coördinates		Bonded to	Key coördinate of neighboring atom
			ρ	ϕ		
C_1	$\frac{11}{16}''$	9 hex	0	0	spacing bar to C_1	$\rho=180$
			90	0	C_2	$\rho=90$
			90	120	C_2	
			90	240	C_2	
			180	0	spacing bar to C_1	$\rho=0$
C_2	$\frac{11}{16}''$	17 hex	0	0	unused	
			90	0	C_1	$\rho=90$
			90	120	C_1	
			90	240	C_1	

A-14, *Iodine*

Atom	Ball Size	Number of balls required for one unit cell model	Drilling Coördinates		Bonded to	Key coördinate of neighboring atom
			ρ	ϕ		
I	$1\frac{3}{8}''$	28	0	0*	spacing bar	$\rho=0$
			90	0	I	$\rho=90$

* This hole is drilled completely through the ball.

A-17, *Black Phosphorus*

Atom	Ball Size	Number of balls required for one unit cell model	Drilling Coördinates		Bonded to	Key coördinate of neighboring atom
			ρ	ϕ		
P	$1\frac{1}{8}''$	36	0	0	space bar to P	$\rho=69$
			69	180	space bar to P	$\rho=0$
			112	$125\frac{1}{2}$	P	$\phi=125\frac{1}{2}$
			112	$234\frac{1}{2}$	P	$\phi=234\frac{1}{2}$
			$125\frac{1}{2}$	0	P	$\rho=125\frac{1}{2}$

B-1, *Halite*

Na	1″	14	0	0	Cl	$\rho=180$
			90	0	Cl	$\rho=90$
			90	90	Cl	
			90	180	Cl	
			90	270	Cl	
			180	0	Cl	$\rho=0$
Cl	$1\frac{13}{16}''$	13	0	0	Na	$\rho=180$
			90	0	Na	$\rho=90$
			90	90	Na	
			90	180	Na	
			90	270	Na	
			180	0	Na	$\rho=0$

B-2, *Caesium Chloride*

Atom	Ball Size	Number of balls required for one unit cell model	Drilling Coördinates		Bonded to	Key coördinate of neighboring atom
			ρ	ϕ		
Cs	$1\frac{3}{4}''$	8	0	0	unused	
			55	0	Cl	$\rho=125$
			55	90	Cl	
			55	180	Cl	
			55	270	Cl	
			125	0	Cl	$\rho=55$
			125	90	Cl	
			125	180	Cl	
			125	270	Cl	
Cl	$1\frac{13}{16}''$	1	0	0	unused	
			55	0	Cs	$\rho=125$
			55	90	Cs	
			55	180	Cs	
			55	270	Cs	
			125	0	Cs	$\rho=55$
			125	90	Cs	
			125	180	Cs	
			125	270	Cs	

B-3, B-4, *Sphalerite and Wurtzite*

Zn	$1\frac{5}{16}''$	14* 11† 20†hex	0	0	S	$\rho=0$
			$109\frac{1}{2}$	0	S	$\rho=109\frac{1}{2}$
			$109\frac{1}{2}$	120	S	
			$109\frac{1}{2}$	240	S	
S	$1\frac{1}{16}''$	12* 10† 19†hex	0	0	Zn	$\rho=0$
			$109\frac{1}{2}$	0	Zn	$\rho=109\frac{1}{2}$
			$109\frac{1}{2}$	120	Zn	
			$109\frac{1}{2}$	240	Zn	

* Sphalerite.
† Wurtzite.

B-5, B-6, B-7, *Carborundum (all modifications)*

Atom	Ball Size	Number of balls required for one unit cell model	Drilling Coördinates		Bonded to	Key coördinate of neighboring atom
			ρ	ϕ		
Si	$1\frac{1}{8}''$	—	0	0	C	$\rho=0$
			$109\frac{1}{2}$	0	C	$\rho=109\frac{1}{2}$
			$109\frac{1}{2}$	120	C	
			$109\frac{1}{2}$	240	C	
C	$\frac{3}{4}''$	—	0	0	Si	$\rho=0$
			$109\frac{1}{2}$	0	Si	$\rho=109\frac{1}{2}$
			$109\frac{1}{2}$	120	Si	
			$109\frac{1}{2}$	240	Si	

B-8, *Niccolite*

Atom	Ball Size	Number of balls required for one unit cell model	Drilling Coördinates		Bonded to	Key coördinate of neighboring atom
			ρ	ϕ		
Ni	$1\frac{1}{4}''$	21 hex	0	0	Ni	$\rho=180$
			59	0	As	$\rho=121$
			59	120	As	
			59	240	As	
			121	60	As	$\rho=59$
			121	180	As	
			121	300	As	
			180	0	Ni	$\rho=0$
As	$1\frac{3}{16}''$	12 hex	0	0	unused	
			59	0	Ni	$\rho=121$
			59	120	Ni	
			59	240	Ni	
			121	0	Ni	$\rho=59$
			121	120	Ni	
			121	240	Ni	

B-8, *Pyrrhotite*

Atom	Ball Size	Number of balls required for one unit cell model	Drilling Coördinates		Bonded to	Key coördinate of neighboring atom
			ρ	ϕ		
Fe	$1\frac{1}{4}''$	21 hex	0	0	S	
			90	0		
			90	90		
			90	180		
			90	270		
			180	0		
S	$1\frac{1}{4}''$	12 hex	0	0	Fe	
			70	0		
			90	$135\frac{1}{2}$		
			90	$224\frac{1}{2}$		
			132	72		
			132	288		

B-9, *Cinnabar* ($u=0.33$, $v=0.21$)

Atom	Ball Size	Number of balls required for one unit cell model	Drilling Coördinates		Bonded to	Key coördinate of neighboring atom
			ρ	ϕ		
Hg	$1\frac{7}{16}''$	16 28 hex	0	0	unused	
			$50\frac{1}{2}$	22	S	$\rho=129\frac{1}{2}$
			90	0	spacing bars to Hg	$\rho=90$
			90	60		
			90	120		
			90	120		
			90	180		
			90	240		
			90	300		
			$129\frac{1}{2}$	338	S	$\rho=50\frac{1}{2}$
S	$1\frac{1}{16}''$	12 21 hex	0	0	unused	
			$50\frac{1}{2}$	38	Hg	$\rho=129\frac{1}{2}$
			$129\frac{1}{2}$	322	Hg	$\rho=50\frac{1}{2}$

B-9, *Cinnabar* ($u=0.72$, $v=0.55$)

Atom	Ball Size	Number of balls required for one unit cell model	Drilling Coördinates ρ	Drilling Coördinates ϕ	Bonded to	Key coördinate of neighboring atom
Hg	$1\frac{7}{16}''$	16 28 hex	0	0	unused	
			$50\frac{1}{2}$	90	S	$\rho=129\frac{1}{2}$
			90 90 90 90 90 90	0 60 120 180 240 300	spacing bars to Hg	$\rho=90$
			$129\frac{1}{2}$	270	S	$\rho=50\frac{1}{2}$
S	$1\frac{1}{16}''$	12 21 hex	0	0	unused	
			$50\frac{1}{2}$	0	Hg	$\rho=129\frac{1}{2}$
			$129\frac{1}{2}$	60	Hg	$\rho=50\frac{1}{2}$

B-11, *PbO*

Pb	$1\frac{5}{8}''$	10	0	0	space bar to Pb	$\rho=0$ $\phi=180$
			121	0	O	
			121	90	O	
			121	180	O	
			121	270	O	
			180	0	space bar to Pb	$\rho=0$ $\phi=0$
O	—	8	0	0(m)	Pb up	$\rho=121$
			$105\frac{1}{2}$	117	Pb down	$\rho=121$
			$105\frac{1}{2}$	243	Pb down	$\rho=121$
			118	0(m)	Pb up	$\rho=121$

"D-31," *Calomel*

Atom	Ball Size	Number of balls required for one unit cell model	Drilling Coördinates		Bonded to	Key coördinate of neighboring atom
			ρ	ϕ		
Hg	$\frac{7}{8}$"	27	0	0	Cl	$\rho=180$
			81	0	Cl	$\rho=81$
			81	90	Cl	
			81	180	Cl	
			81	270	Cl	
Cl	$1\frac{5}{8}$"	27	0	0	Cl	$\rho=0$
			81	0	Hg	$\rho=81$
			81	90	Hg	
			81	180	Hg	
			81	270	Hg	
			180	0	Hg	$\rho=0$

B-12, *Boron nitride*

Atom	Ball Size	Number of balls required for one unit cell model	Drilling Coördinates		Bonded to	Key coördinate of neighboring atom
			ρ	ϕ		
B	$\frac{3}{4}$"	17 hex	0	0	unused	
			90	0	N	$\rho=90$
			90	120	N	
			90	240	N	
N	$\frac{11}{16}$"	9 hex	0	0	spacing bar to N	$\rho=180$
			90	0	B	$\rho=90$
			90	120	B	
			90	240	B	
			180	0	spacing bar to N	$\rho=0$

B-18, *Covellite*

Atom	Ball Size	Number of balls required for one unit cell model	Drilling Coördinates		Bonded to	Key coördinate of neighboring atom
			ρ	ϕ		
Cu_I	$1\frac{1}{8}''$	12 hex	0	0	unused	
			90	0	S_I	$\rho=90$
			90	120	S_I	
			90	240	S_I	
S_I	$1\frac{1}{16}''$	12 hex	0	0	Cu_{II}	$\rho=0$
			90	0	Cu_I	$\rho=90$
			90	120	Cu_I	
			90	240	Cu_I	
			180	0	Cu_{II}	$\rho=0$
Cu_{II}	$1\frac{5}{16}''$	24 hex	0	0	S_I	$\rho=0$ or $\rho=180$
			109	0	S_{II}	$\rho=109$
			109	120	S_{II}	
			109	240	S_{II}	
S_{II}	$1''$	28 hex	0	0	S_{II}	$\rho=0$
			109	0	Cu_{II}	$\rho=109$
			109	120	Cu_{II}	
			109	240	Cu_{II}	

B-17, *Cooperite*

Pt	$1\frac{1}{4}''$	14 C	0	0	unused	
			90	0	S	$\rho=131$
			90	98	S	
			90	180	S	$\rho=49$
			90	278	S	
S	$1\frac{1}{16}''$	32 C	0	0	unused	
			49	0	Pt	$\rho=90$
			49	180	Pt	
			131	90	Pt	
			131	270	Pt	

B-26, *Tenorite*

Atom	Ball Size	Number of balls required for one unit cell model	Drilling Coördinates		Bonded to	Key coördinate of neighboring atom
			ρ	ϕ		
Cu	$1\frac{1}{4}''$	14	0	0	unused	
			90	0	O	
			90	85	O	
			90	180(m)*	O	
			90	265(m)*	O	
O_R	$\frac{11}{16}''$	16	0	0(m)*	Cu	
			96	107	Cu	
			104	260	Cu	
			108	0(m)*	Cu	
O_L	$\frac{11}{16}''$	16	0	0(m)*	Cu	
			96	253	Cu	
			104	100	Cu	
			108	0(m)	Cu	

* Make *one mark between* these pairs of holes.

C-1, *Fluorite*

Ca	1″	14	0	0	unused	
			55	0	F	$\rho=125$
			55	90	F	
			55	180	F	
			55	270	F	
			125	0	F	$\rho=55$
			125	90	F	
			125	180	F	
			125	270	F	
F	$1\frac{3}{8}''$	8	0	0	unused	
			55	0	Ca	$\rho=125$
			55	180	Ca	
			125	90	Ca	$\rho=55$
			125	270	Ca	

C-2, *Pyrite*

Atom	Ball Size	Number of balls required for one unit cell model	Drilling Coördinates		Bonded to	Key coördinate of neighboring atom
			ρ	ϕ		
Fe	$1\frac{3}{16}''$	14	0	0	unused	
			58	0	S	$\rho = 102\frac{1}{2}$
			58	120	S	
			58	240	S	
			122	60	S	$\rho = 102\frac{1}{2}$
			122	180	S	
			122	240	S	
S	$1\frac{1}{16}''$	26	0	0	S	$\rho = 0$
			$102\frac{1}{2}$	0	Fe	$\rho = 58$ or
			$102\frac{1}{2}$	120	Fe	$\rho = 122$
			$102\frac{1}{2}$	240	Fe	

C-3, *Cuprite*

Atom	Ball Size	Number of balls required for one unit cell model	Drilling Coördinates		Bonded to	Key coördinate of neighboring atom
			ρ	ϕ		
Cu	$\frac{5}{8}''$	4	0	0	O	$\rho = 125$
			180	0	O	$\rho = 55$
O	$1\frac{1}{4}''$	9	0	0	spacing bar to O	$\rho = 180$
			55	0	Cu	$\rho = 180$
			55	180	Cu	
			125	90	Cu	$\rho = 0$
			125	270	Cu	
			180	0	spacing bar to O	$\rho = 0$

C-4, *Rutile*

Atom	Ball Size	Number of balls required for one unit cell model	Drilling Coördinates		Bonded to	Key coördinate of neighboring atom
			ρ	ϕ		
Ti	$\frac{3}{4}''$	9	0	0	O	$\rho=0$
			90	0	O	$\rho=128\frac{1}{2}$
			90	$77\frac{1}{2}$	O	
			90	180	O	
			90	$257\frac{1}{2}$	O	
			180	0	O	$\rho=0$
O	$1\frac{1}{4}''$	6	0	0	Ti	$\rho=0$
			$128\frac{1}{2}$	0	Ti	$\rho=90$
			$128\frac{1}{2}$	180	Ti	
			180	0	O	$\rho=180$

C-5, *Anatase*

Atom	Ball Size	Number of balls required for one unit cell model	Drilling Coördinates		Bonded to	Key coördinate of neighboring atom
			ρ	ϕ		
Ti	$\frac{3}{4}''$	13	0	0	O	$\rho=0$
			78	0	O	$\rho=102$
			78	180	O	
			102	90	O	
			102	270	O	
			180	0	O	$\rho=0$
O	$1\frac{1}{4}''$	22	0	0	Ti	$\rho=0$ or $\rho=180$
			$50\frac{1}{2}$	0	O	$\rho=50\frac{1}{2}$
			$50\frac{1}{2}$	180	O	
			102	0	Ti	$\rho=78$ or
			102	180	Ti	$\rho=102$

C-6, *Tin Disulfide* (covalent bond model)

Atom	Ball Size	Number of balls required for one unit cell model	Drilling Coördinates		Bonded to	Key coördinate of neighboring atom
			ρ	ϕ		
Sn	$1\frac{1}{2}''$	14	0	0	S	$\rho = 0,90$
			$54\frac{3}{4}$	45	Sn	$\rho = 54\frac{3}{4}$
			90	0	S	$\rho = 0,90$
			90	90		
			90	180		
			90	270		
			180	0		
S	$1\frac{1}{16}''$	48	0	0	Sn	$\rho = 0, 90, 180$
			90	0		
			90	90		

C-6, *Tin Disulfide* (ionic bond model)

Atom	Ball Size	Number of balls required for one unit cell model	Drilling Coördinates		Bonded to	Key coördinate of neighboring atom
			ρ	ϕ		
Sn	$\frac{11}{16}''$	12	0	0	S	$\rho = 54\frac{3}{4}°$
S	$1\frac{3}{4}''$	24	0	0	not used	
			35	30	S	$\rho = 145\frac{1}{4}$
			$54\frac{3}{4}$	90	Sn	$\rho = 0$
			90	0	S	$\rho = 90$
			90	60		
			90	120		
			90	180		
			90	240		
			90	300		
			$145\frac{1}{4}$	90	S	$\rho = 54\frac{3}{4}$

C-7, *Molybdenite*

Atom	Ball Size	Number of balls required for one unit cell model	Drilling Coördinates		Bonded to	Key coördinate of neighboring atom
			ρ	ϕ		
Mo	$1\frac{5}{16}''$	20 hex	0	0	spacing bar to S	$\rho=0$
			50	0	S	$\rho=130$
			50	120	S	
			50	240	S	
			130	0	S	
			130	120	S	
			130	240	S	
S	$1\frac{1}{16}''$	38 hex	0	0	spacing bar to Mo	$\rho=0$
			130	0	Mo	$\rho=50$ or $\rho=130$
			130	120	Mo	
			130	240	Mo	

C-18, *Marcasite*

Atom	Ball Size	Number of balls required for one unit cell model	Drilling Coördinates		Bonded to	Key coördinate of neighboring atom
			ρ	ϕ		
Fe	$1\frac{1}{8}''$	12	0	0	S	$\rho=103\frac{1}{2}$
			89	49(m)	S	$\rho=106\frac{1}{2}$
			89	311(m)	S	
			91	131	S	
			91	229	S	
			180	0	S	$\rho=103\frac{1}{2}$
S	$1\frac{1}{8}''$	12	0	0	S	$\rho=0$
			$103\frac{1}{2}$	0(m)	Fe	$\rho=0$ or $\rho=180$
			$106\frac{1}{2}$	$128\frac{1}{2}$	Fe	$\rho=89$ or $\rho=91$
			$106\frac{1}{2}$	$231\frac{1}{2}$	Fe	

C-18, *Löllingite*

Atom	Ball Size	Number of balls required for one unit cell model	Drilling Coördinates		Bonded to	Key coördinate of neighboring atom
			ρ	ϕ		
Fe	$1\frac{1}{8}''$	9	0	0	As	$\rho=108$ $\phi=0$
			88 88 92 92	142(m) 218(m) 38 312	As As As As	$\rho=108$ $\phi=140, 220$
			180	0	As	$\rho=108$ $\phi=0$
As	$1\frac{1}{4}''$	12	0	0	As	$\rho=0$
			108	0(m)	Fe	$\rho=0$ or $\rho=180$
			108 108	140 220	Fe Fe	$\rho=88$ or $\rho=92$

C-18, *Iron di-phosphide*

Atom	Ball Size	Number of balls required for one unit cell model	Drilling Coördinates		Bonded to	Key coördinate of neighboring atom
			ρ	ϕ		
Fe	$1\frac{1}{8}''$	9	0	0	P	$\rho=110\frac{1}{2}$
			88 88 92 92	145(m) 215(m) 35 325	P P P P	$\rho=107$
			180	0	P	$\rho=110\frac{1}{2}$
P	$1\frac{1}{8}''$	12	0	0	P	$\rho=0$
			$110\frac{1}{2}$	0(m)	Fe	$\rho=0$ or $\rho=180$
			107 107	143 217	Fe Fe	$\rho=88$ or $\rho=92$

C-18, *Iron di-antimonide*

Atom	Ball Size	Number of balls required for one unit cell model	Drilling Coördinates		Bonded to	Key coördinate of neighboring atom
			ρ	ϕ		
Fe	$1\frac{1}{4}''$	9	0	0	Sb	$\rho=107$
			88	$142\frac{1}{2}$(m)	Sb	$\rho=108$
			88	$217\frac{1}{2}$(m)	Sb	
			92	$37\frac{1}{2}$	Sb	
			92	$322\frac{1}{2}$	Sb	
			180	0	Sb	$\rho=107$
Sb	$1\frac{3}{8}''$	12	0	0	Sb	$\rho=0$
			107	0(m)	Fe	$\rho=0$ or $\rho=180$
			108	140	Fe	$\rho=88$ or
			108	220	Fe	$\rho=92$

C-18 (C-35), *Hydrophilite*

Atom	Ball Size	Number of balls required for one unit cell model	Drilling Coördinates		Bonded to	Key coördinate of neighboring atom
			ρ	ϕ		
Ca	$1\frac{1}{4}''$	9	0	0	Cl	$\rho=0$
			90	50(m)	Cl	$\rho=128$
			90	310(m)	Cl	
			90	130	Cl	
			90	230	Cl	
			180	0	Cl	$\rho=0$
Cl	$1\frac{1}{2}''$	8	0	0	Ca	$\rho=0$
			128	80	Ca	$\rho=90$
			128	280	Ca	

C-42, *Silicon di-sulphide*

Atom	Ball Size	Number of balls required for one unit cell model	Drilling Coördinates		Bonded to	Key coördinate of neighboring atom
			ρ	ϕ		
Si_R	$1\frac{1}{8}''$	9	0	0*	spacing bar	
			50 50	0 180	S S	$\rho=0$
			130 130	94 274	S S	$\rho=0$
Si_L	$1\frac{1}{8}''$	6	0	0*	spacing bar	
			50 50	0 180	S S	$\rho=80$
			130 130	86 266	S S	$\rho=80$
S_R, S_L	$1\frac{1}{16}''$	20	0 80	0 0	Si_R Si_L	$\rho=50$ or $\rho=130$

* Hole is drilled completely through the ball.

C-9, *High Cristobalite*

Atom	Ball Size	Number of balls required for one unit cell model	Drilling Coördinates		Bonded to	Key coördinate of neighboring atom
			ρ	ϕ		
O	$1\frac{1}{4}''$	56	0	0	unused	
			35 35 35	0 120 240	O O O	$\rho=35$
			145 145 145	60 180 300	O O O	$\rho=145$
Si	.30″	18	—	—	—	

C-30, *Low Cristobalite*

Atom	Ball Size	Number of balls required for one unit cell model	Drilling Coördinates		Bonded to	Key coördinate of neighboring atom
			ρ	ϕ		
O	$1\frac{5}{16}''$	56	0	0	unused	
			$48\frac{1}{2}$	$69\frac{1}{2}$	O	$\rho = 131\frac{1}{2}$
			66	0	O	$\rho = 66$
			$104\frac{1}{2}$	47	O	$\rho = 104\frac{1}{2}$ $\phi = 223$
			$104\frac{1}{2}$	223	O	$\rho = 104\frac{1}{2}$ $\phi = 47$
			$131\frac{1}{2}$	$160\frac{1}{2}$	O	$\rho = 48\frac{1}{2}$
			156	270	O	$\rho = 156$
Si	.30″	18	—	—	—	

C-10, *High Tridymite*

O_I	$1\frac{1}{4}''$	42 72 hex	0	0	unused	
			35	0	O_{II}	$\rho = 145$
			35 35	120 240	O_I O_I	$\rho = 35$
			145	60	O_I	$\rho = 145$
			145	180	O_{II}	$\rho = 35$
			145	300	O_I	$\rho = 145$
O_{II}	$1\frac{1}{4}''$	14 24 hex	0	0	unused	
			35 35 35	0 120 240	O_I O_I O_I	$\rho = 145$
			145 145 145	0 120 240	O_I O_I O_I	$\rho = 35$
Si	.30″	21 36 hex	—	—	—	

C-8, *High Quartz*

Atom	Ball Size	Number of balls required for one unit cell model	Drilling Coördinates		Bonded to	Key coördinate of neighboring atom
			ρ	ϕ		
O	$1\frac{5}{16}''$	38	0	0	unused	
			35	0	O	$\rho=135$
			35	120	O	$\rho=35$ $\phi=120$
			35	240	O	$\rho=124$
			124	305	O	$\rho=35$ $\phi=240$
			135	225	O	$\rho=35$ $\phi=0$
			165	45	O	$\rho=165$
Si	.30″	12	—	—	—	

"C-8," *Low Quartz*

O	$1\frac{5}{16}''$	38	0	0	unused	
			48	$167\frac{1}{2}$	O	$\rho=132$
			$63\frac{1}{2}$	240	O	$\rho=63\frac{1}{2}$
			103	$46\frac{1}{2}$	O	$\rho=103$ $\phi=193\frac{1}{2}$
			103	$193\frac{1}{2}$	O	$\rho=103$ $\phi=46\frac{1}{2}$
			132	$107\frac{1}{2}$	O	$\rho=48$
			$153\frac{1}{2}$	0	O	$\rho=153\frac{1}{2}$
Si	.30″	12	—	—	—	

STUDIES IN MINERAL FLUORESCENCE

EDWARD S. C. SMITH AND WILLIAM H. PARSONS,
Union College, Schenectady, N. Y.

ABSTRACT

Availability of an unusual instrument giving monochromatic radiant energy of a higher order of magnitude than hitherto possible has permitted the pursuit of this research. Specimens of forty-three minerals representing twenty-one distinct species have been examined in ultraviolet radiation and a tentative relationship between the frequency of the incident radiation and the frequency of the reradiated light has been determined.

Fluorescence in minerals has been a commonly known phenomenon for many years, and during the last five years mineralogists have had access to various sources of ultraviolet radiation, as for example the argon tube. This has resulted in the demonstration of fluorescence in an increasingly large number of the mineral species and in the awakening of wide-spread interest in this property.

To obtain a range of frequencies in the ultraviolet the practice of other workers has followed three methods. The first has been to remove the plate holder from a prism, or diffraction grating spectrograph, and to allow monochromatic radiation to fall upon the specimen. This process is subject to great calibration difficulties and with interference from scattered light of other frequencies present nearby, especially the visible lines. While this method is suitable for chemical compounds which may be spread out in a thin layer on a glass plate, it is unsatisfactory for examination of the rather rough surfaces of minerals, particularly those species which lose the characteristic fluorescent response when pulverized.

A second way to secure monochromatic radiation has been through the use of specially made glass filters which allow only certain ranges of frequencies to pass. Here one is subject to the obvious difficulty of getting a sufficiently wide assortment of frequencies having sharp cut-off limitations, although the radiation intensity is comparatively strong.

Monochromators using prisms made from natural crystals of quartz seriously limit the transmitted radiant energy because of the necessary size restriction of the cut prisms.

The type of paper usually found in the literature makes it evident that investigators have been limited in facilities for measuring fluorescent responses under a suitable range of frequencies.

The reason for the study, the results of which appear in this paper, has been the availability, through the courtesy of its designer, Mr. Frank A. Benford of the Research Laboratory of the General Electric

Company, at Schenectady, N.Y., of an unique monochromator of the following construction.

Fused quartz prisms weighing approximately seven and ten pounds each, which have optical surfaces of the order of ten and fifteen centimeters on a side respectively, turn on their axes by means of revolving tables, being actuated simultaneously. A revolving drum scale is attached permitting the setting of the instrument at the desired frequency. There are two sets of quartz collimating lenses. The light source is a mercury vapor arc in quartz operating at 150 volts and 3.6 amperes, being kept at constant temperature by a stream of air directed upon it, thus maintaining a constant energy output.

It is important to note the special design of the fused quartz prisms. They are not entirely free from bubbles and striae and therefore scattered light is present in small amounts. But by an ingenious design of their angles it has been possible to divert from the optical system much energy from those wavelengths longer than the one in use at any given time. These are naturally the wavelengths of greater energy and would be especially undesirable lest they mask the fluorescent effect when tests are made near the visible range.

The monochromator is unique primarily in that it gives radiant energy of a much greater order of magnitude than that of instruments heretofore in use, enabling the easy examination of large irregular surfaces at a given wavelength.

It was decided to make the selection of minerals as complete as possible, hence a collection of several thousand specimens was tested for fluorescence with both mercury lamp and disruptive iron spark radiations. Forty-three specimens representing twenty-one distinct species were finally chosen for study. Each mineral was examined through the range of ultraviolet frequencies available from the monochromator and the following table prepared (Table 1).

TABLE 1

Wavelength	Relative energy (% of lamp input)	Sphalerite ZnS Tsumeb, Africa	Fluorite CaF_2 St. Lawrence, Co., N.Y.	Fluorite (brown) CaF_2 Ohio	Fluorite (yellow) CaF_2 Ohio	Fluorite CaF_2 Montana	Fluorite (blue) CaF_2 England	Fluorite (green) CaF_2 England	Semi-opal $SiO_2 \cdot nH_2O$ Nevada
2652Å	.0005	3 orange	0	3 brown	1 brown-green	2 blue	2 blue-violet	2 violet	6 green
2700Å	.0008	4 orange	0	3 brown	1 brown-green	2 blue	2 blue-violet	2 violet	7 green
2752Å	.0010	5 orange	0	3 brown	1 brown-green	2 blue	2 blue-violet	2 violet	7 green
2804Å	.0016	5 orange	0	3 brown	2 brown-green	2 blue	3 blue-violet	2 violet	8 green
2894Å	.0010	5 orange	0	3 brown	2 brown-green	1 blue	3 blue	3 blue	6 green
2925Å	.0005	5 orange	0	3 brown	2 brown-green	2 blue	4 blue	4 blue	6 green
2967Å	.0025	5* orange	0	4 brown	3 brown-green	3 blue	5 blue	4 blue	6 green
3024Å	.0063	5* orange	3 blue	4 brown-green	3 brown-green	4 blue	6 blue	5 blue	7 green
3128Å	.0130	6* orange	4 blue	5 brown-green	4 brown-green	4 blue	7 blue	6 blue	7 green
3341Å	.0030	6* orange	4 blue	3 brown-green	2 brown-green	5 blue	8 blue	8 blue	5 green
3650Å	.0235	8* orange	5 blue	5 brown-green	4 brown-green	7 blue	9 blue	9 blue	6 green
4047Å	.0100	6* orange	5 blue	5 brown-green	2 brown-green	?	8 blue	8 blue	5 green
4358Å	.0140	6* orange	?	?	?	?	?	?	?

* Phosphorescence.
? Response doubtful.

TABLE 1 (*Continued*)

Wavelength	Hyalite $SiO_2 \cdot nH_2O$ Mexico	Hyalite $SiO_2 \cdot nH_2O$ North Carolina	Ruby Al_2O_3 North Carolina	Brucite $Mg(OH)_2$ Texas, Pa.	Brucite $Mg(OH)_2$ Hoboken, N.J.	Calcite $CaCO_3$ Montana	Calcite $CaCO_3$ Chisos Mtns., Texas	Calcite $CaCO_3$ Imperial Co., Calif.	Calcite (green) $CaCO_3$ California
2652Å	8 green	8 blue-green	0	0	1 light blue	0	5* blue	0	0
2700Å	7 green	8 blue-green	0	0	1 light blue	0	2* blue	0	0
2752Å	7 green	7 blue-green	0	1 light blue	1 light blue	0	2* blue	0	0
2804Å	8 green	8 blue-green	0	1 light blue	1 light blue	0	4* blue	0	1 pink
2894Å	6 green	7 blue-green	0	1 light blue	1 light blue	0	4* blue	0	1 pink
2925Å	5 green	7 green	0	2 light blue	2 light blue	0	3* blue	0	1 pink
2967Å	6 green	7 green	0	2 light blue	2 light blue	0	5* blue	0	1 pink
3024Å	7 green	8 green	0	3 light blue	3 light blue	0	5* blue	1 red	2 red
3128Å	7 green	8 green	0	3 light blue	4 light blue	0	4* blue	2 red	3 red
3341Å	5 green	7 green	0	3 light blue	4 light blue	0	0	2 red	3 red
3650Å	6 green	7 green	4 red	6 light blue	7 light blue	1? red	7 pink	4 red	5 red
4047Å	2 green	6 green	5 red	3? light blue	3? light blue	?	4 pink	5 red	5 red
4358Å	?	?	?	?	?	?	?	?	?

* Phosphorescence.
? Response doubtful.

TABLE 1 (*Continued*)

Wavelength	Calcite $CaCO_3$ Sterlingbush, N.Y.	Calcite $CaCO_3$ Saxony	Calcite $CaCO_3$ Devonshire, Eng.	Calcite $CaCO_3$ Franklin Furnace, N.J.	Calcite $CaCO_3$ Franklin Furnace, N.J.	Calcite $CaCO_3$ Franklin Furnace, N.J.	Dolomite $(Ca, Mg)CO_3$ Baden, Germany	Gay-Lussite $CaCO_3 \cdot Na_2CO_3 \cdot 5H_2O$ Washington	Kunzite $LiAl(SiO_3)_2$ California
2652Å	0	2 pink	1 pink	6 pink	3 pink	4 orange-pink	2 green	0	0
2700Å	0	3 pink	2 pink	6 pink	3 pink	4 orange-pink	3 green	0	0
2752Å	1 pink	4 pink	3 pink	6 pink	4 pink	6 pink	3 green	3 pink	0
2804Å	5 pink	5 pink	4 pink	8 pink	4 pink	6 pink-orange	3 green	3 pink	0
2894Å	5 orange-pink	5 pink	4 pink	7 pink	4 pink	6 pink-orange	1 green	2 pink	0
2925Å	4 orange-pink	6 pink	4 pink	7 pink	5 pink-orange	7 orange	1 green	3 pink	0
2967Å	6 orange-pink	7 pink	5 pink	7 orange-pink	5 orange	7 orange	1 green	3 pink	0
3024Å	7 orange-pink	7 pink	7 pink	8 orange	7 orange	8 orange	1 green	4 pink	0
3128Å	5 orange-pink	8 pink	8 pink	9 orange	8 orange	9 orange	0	5 pink	0
3341Å	1 orange-pink	3 pink	2 pink	7 orange	4 orange-pink	6 orange	0	4 pink	1 orange
3650Å	2 orange-pink	3 pink	4 pink	5 orange	6 orange-pink	7 pink-orange	0	4 pink	4 orange
4047Å	?	2 pink	8 pink	5 orange	7 orange-pink	7 orange-pink	0	?	4 orange
4358Å	?	?	?	?	?	?	?	?	?

* Phosphorescence.

? Response doubtful.

TABLE 1 (*Continued*)

Wavelength	Pectolite $HNaCa_2(SiO_3)_3$ Paterson, N.J.	Sodalite $Na_4(Al, Cl)Al_2(SiO_4)_3$ Brewig, Norway	Hackmanite Complex Silicate Bancroft, Ontario	Willemite Zn_2SiO_4 Franklin Furnace, N.J.	Willemite (crystals) Zn_2SiO_4 Sterling, N.J.	Scapolite Complex Silicate Quebec	Wavellite $4AlPO_4 \cdot 2Al(OH)_3 \cdot 9H_2O$ Devonshire, Eng.	Autunite $Ca(UO_2)_2P_2O_8 \cdot 8H_2O$ Chesterfield, Mass.	Autunite $Ca(UO_2)_2P_2O_8 \cdot 8H_2O$ Grafton, N.H.
2652Å	0	0	0	8 green	4 green	3 yellow-orange	0	5 green	6 green
2700Å	0	0	0	8 green	4 green	4 yellow-orange	0	5 green	6 green
2752Å	0	0	0	9 green	4 green	4 yellow-orange	0	5 green	6 green
2804Å	0	0	0	9 green	4 green	5 yellow	0	6 green	7 green
2894Å	0	0	0	9 green	3 green	5 yellow	0	6 green	7 green
2925Å	0	0	0	9 green	2 green	5 yellow	0	6 green	8 green
2967Å	0	0	1 pink	9 green	2 green	6 yellow	0	7 green	8 green
3024Å	0	0	1 pink	9 green	2 green	7 yellow	1 green	7 green	9 green
3128Å	0	0	2 pink	8 green	0	7 yellow	1 green	7 green	9 green
3341Å	0	0	2 pink	7 green	0	7 yellow	1 green	4 green	8 green
3650Å	1 orange	4 pink	5 orange-pink	8 green	0	10 yellow	3* light green	6 green	9 green
4047Å	0	4 pink	6 orange-pink	0	0	9 yellow	1* light green	0	7 green
4358Å	?	?	5 orange-pink	5 green	0	9 yellow-orange	?	?	?

* Phosphorescence.

? Response doubtful.

TABLE 1 (*Continued*)

Wavelength	Autunite $Ca(UO_2)_2P_2O_8 \cdot 8H_2O$ Autun, France	Barite $BaSO_4$ Przibram, Bohemia	Barite $BaSO_4$ Schemnitz, Hungary	Anglesite $PbSO_4$ Phoenixville, Pa.	Gypsum $CaSO_4 \cdot 2H_2O$ Bennett Co., S.D.	Gypsum $CaSO_4 \cdot 2H_2O$ Chicago, Ill.	Scheelite $CaWO_4$ Bohemia	Scheelite $CaWO_4$ California
2652Å	7 green	1 blue	0	1 green-yellow	0	0	4 blue	8 blue
2700Å	7 green	1 blue	1 light green	1 green-yellow	1 yellow-orange	0	5 blue	7 blue
2752Å	7 green	1 blue	1 light green	2 green-yellow	1 yellow-orange	0	6 blue	7 blue
2804Å	8 green	1 blue	1 light green	2 green-yellow	1 yellow-orange	1 blue	7 blue	8 blue
2894Å	8 green	0	1 light green	2 green-yellow	1 yellow-orange	0	3 blue	6 blue
2925Å	8 green	0	1 light green	2 green-yellow	1 yellow-orange	0	1 blue	4 blue
2967Å	8 green	0	2 light green	3 green-yellow	1 yellow-orange	1 blue	1 blue	2 blue
3024Å	9 green	1 blue	2 light green	3 green-yellow	2 yellow-orange	1 blue	0	0
3128Å	9 green	2 blue-green	2 light green	4 green-yellow	3 yellow	2 blue	0	0
3341Å	8 green	1 green	1 light green	3 green-yellow	2 yellow	1 blue	0	0
3650Å	9 green	2 yellow-cream	1 light green	5 green-yellow	4 orange-yellow	2 blue-green	0	0
4047Å	8 green	0	0	2 yellow	3 orange-yellow	?	0	0
4358Å	7? green	0	0	?	?	?	?	?

* Phosphorescence.

? Response doubtful.

With reference to these observations, the subject of the intensity of fluorescent light from the specimen deserves primary consideration. For a given specimen the relationship between incident radiant energy and fluorescent light energy is not a linear one. This fact may be made evident by the simple experiment of doubling the incident energy at a given frequency and observing the increase in fluorescence. This may be appreciable but fluorescence will rarely approximate twice its former value. Therefore, large variations in the strength of a given line produce rather small changes in fluorescent light from the specimen. There is probably some phenomenon of absorption operative here. To establish this relationship is difficult. Variations of incident energy from the monochromator with each successive spectral line make it, therefore, of little avail to measure fluorescent response in absolute units. Thus, instead of using a photocell or thermopile for quantitative measurements, the table is derived from visual estimation.

A zero rating indicates no fluorescence while optimum brightness is recorded as ten units. Thus "1" indicates a barely discernible fluorescence while "5" or "6" is perhaps the average value. Color is indicated on the table for each response. Phosphorescence is shown by an appropriate symbol.

It is extremely important always to interpret the recorded intensities as dependent upon the energy of each ultraviolet wavelength.

Attention is first directed to those specimens which undergo color changes. There are nine minerals in which the change is definitely observable. They are:

Minerals	(*Incident radiation decreases in frequency*)
Fluorite (brown) Ohio	brown to brown-green
Fluorite (blue) England	blue-violet to blue
Fluorite (green) England	violet to blue-violet
Hyalite North Carolina	blue-green to green
Calcite Texas	blue to pink
Barite Bohemia	blue to blue-green to green to yellow-green
Anglesite Phoenixville, Pa.	green-yellow to yellow
Gypsum Chicago, Ill.	blue to blue-green

We note at once an important fact. In every instance above, the wavelength of the fluorescent color varies directly with the wavelength of the incident ultraviolet radiation. In other words, the higher the frequency of the ultraviolet radiation, the higher the frequency of the reradiated energy.

Opposed to this group is a series which tends to show the opposite effect. This is composed of:

Minerals	(*Incident radiation decreases in frequency*)
Calcite Sterlingbush, N.Y.	pink to orange-pink
Calcite Franklin Furnace, N.J.	pink to orange-pink
Hackmanite Bancroft, Ontario	pink to orange-pink
Scapolite Ontario	yellow-orange to yellow to yellow-orange (?)

Here it would seem as if the incident frequency and reradiated frequency varied in inverse proportion. However, the above four specimens are not clearcut examples, due to the difficulty in describing what really amounts to a slight gradation of shading. This evidence, therefore, is not given extensive consideration.

The third and largest group contains the remaining specimens, those which show no appreciable change in color under the entire range of incident frequencies. It will be noted that a specimen may show fluorescence of but one color under a certain incident frequency, yet fail to respond at all to other nearby incident frequencies which one might expect to produce adjacent spectral colors in the visible range.

Two conclusions may be made in reference to the species examined. The frequency of the fluorescent light is a discontinuous function of the frequency of the incident radiation. Further, within limited regions where specimens show that it is a continuous function, the frequency of fluorescent color varies directly as the frequency of the incident ultraviolet radiation. This mutual variation is not a direct octave relationship nor is it a linear one, for any specimen studied.

SUPPLEMENTARY NOTES ON AXINITE

M. A. Peacock, *University of Toronto, Toronto, Canada.*

The following notes supplement a recent paper (1937) on the crystallography of axinite. The question of symmetry was purposely not broached in the original paper since the issue seemed unclear. The new forms and confirmatory measurements have only recently become available. The remaining points refer to more or less inaccessible observations which had escaped my notice. For calling attention to the two neglected settings of axinite by Fedorov full credit is due to Professor Wartan N. Lodočnikow of Leningrad, who was also kind enough to refer me to his paper (1927) describing twinning and a new form on axinite.

Symmetry

Despite the fact that there are several early notices of a positive pyroelectric effect in axinite (Hintze, 1897), pointing to the absence of a symmetry centre and therefore to the pedial (hemihedral) class of the triclinic system, axinite is generally accepted as belonging to the pinakoidal (holohedral) class and was given as such by the present writer. This contradiction was realized at the time and an effort was made to obtain new observations which might decide the question. Crystals of axinite from near Easton, Pennsylvania and mangan-axinite from Franklin, New Jersey, were sent to Dr. Sterling B. Hendricks, Bureau of Chemistry and Soils, Washington, D.C., who kindly undertook to make tests for pyro- and piezoelectricity, using recently described methods. The following are excerpts from Dr. Hendricks' privately communicated reports:

> Jefferson tested the piezoelectric character of the two axinite specimens, using an oscillator of the type recommended by Giebe and Scheibe [1925]. The result was negative under conditions that gave a positive test on meta nitro aniline which shows a weak piezoelectric behaviour. I tested the pyroelectric character after the Martin [1931] method. . . . A negative result was obtained under conditions that gave positive results for alunite and jarosite.—Jan. 26, 1937.
>
> I was aware that axinite has been described as being pyroelectric and I for one think that the former tests are correct. . . . We place absolutely no faith in the tests [Giebe and Scheibe; Martin] or in our ability of applying them. However we always make them since a positive result is undeniable.—Feb. 4, 1937.

Thus, although Dr. Hendricks made it clear that negative pyro- and piezoelectric tests are valueless, it seemed that the early positive result lacked confirmation and that, therefore, there was insufficient ground for questioning the accepted pinakoidal symmetry of axinite.

It was overlooked, however, that Martin himself (1931) reported a positive pyroelectric effect in axinite, thus confirming the early work. Since a positive result is undeniable we must, according to accepted theory, place axinite in the pedial class in which each form is represented by a single plane (pedion). Although it might prove possible, by an extended research, to fix the position of a unique polar axis in axinite and separate the apparently pinakoidal forms into positive and negative pedions, this would be a difficult and perhaps unprofitable undertaking.

Crystallographic Settings

In addition to the seventeen settings of axinite previously discussed or briefly mentioned (1937), three more have come to the writer's attention: two by Fedorov, much of whose valuable work is inaccessible in America, and one by Schiebold who gives lattice dimensions for axinite in a new setting in a long footnote to an extended paper on the feldspars.

Fedorov (1901): In his earlier setting Fedorov treats axinite as a hypo-hexagonal species with a four-index notation. It would be difficult to derive the transformation to the normal setting in this case, and of little value, since Fedorov later abandoned the hypo-hexagonal setting in favour of a happier orientation.

Fedorov (1920): In his monumental work *Das Krystallreich* Fedorov treats axinite as a hypo-cubic species and relates his setting to that of Dana (1892) by the transformation:

Dana to Fedorov: $\bar{2}00/002/110$

Since the transformation Peacock to Dana is $010/2\bar{1}0/001$ (Donnay, 1937) we have, by multiplication of matrices, Peacock to Fedorov: $01\bar{0}/001/\bar{1}00$, giving the inverse transformation:

Fedorov to Peacock: $00\bar{1}/\bar{1}00/010$

This transformation simply represents an interchange of axes; and thus we see that, in this case, Fedorov's "richtige Aufstellung" is the same as the writer's "normal setting" except in the purely arbitrary matter of naming the axes of the lattice cell.

Schiebold (1931): This setting, given by structural lattice dimensions which will be considered later, can be related to ours only if we assume that Schiebold's axial angle $\gamma = [100]:[010]$ is the supplement of the proper value. Such errors are common in the literature of axinite. In that case the transformation is:

Schiebold to Peacock: $00\bar{1}/010/100$

which likewise simply represents an interchange of axes.

Thus, in all, we have six settings of the correct lattice cell: Miller (1852), Goldschmidt (1886), Goldschmidt (1897), Fedorov (1920) Schiebold (1931), Peacock (1937). This clearly shows how important it is to follow some simple rules, as proposed in the normal setting, that admit only one of the twenty-four orientations in which a given triclinic cell may be placed.[1]

Fundamental Angles

In an extended work on the morphology of axinite, which appeared while the writer's paper was in press, Heritsch (1937) tabulates the mean values for a series of new measurements on four of the principal forms on axinite crystals from six localities. Heritsch uses the orientation of Goldschmidt (1897) which is related to ours by the transformation:

Goldschmidt to Peacock: $\bar{1}00/0\bar{1}0/001$

Heritsch's angles compare with the calculated values of Miller (Goldschmidt, 1897) and Palache (Peacock, 1937) as follows:

Heritsch			Miller (Gdt.)		Palache		
Form	$180°-\phi$	ρ	$180°-\phi$	ρ	Form	ϕ	ρ
a 101	− 75°52′	49°09′	− 75°56′	49°10′	y $\bar{1}01$	− 75°45½′	49°13½′
o 112	−126 08	31 14	−126 11	31 19	o $\bar{1}\bar{1}2$	−126 01	31 16
x $1\bar{1}1$	− 41 10	59 35	− 41 12	59 36	x $\bar{1}11$	− 41 09	59 39½
s $\bar{1}2\bar{1}$	− 26 09	68 33	− 26 11	68 32	s $\bar{1}21$	− 26 10	68 34½

The three sets of angles are very nearly alike and thus we have confirmation of the accuracy of Palache's definitive elements which were based on a judicious combination of many old and new measurements.

Forms

From Heritsch's careful study we may add four well established new forms to Palache's list:

$K_0\{3\bar{2}0\}$ Heritsch = $K:\{3\bar{2}0\}$ Palache
I $\{212\}$ Heritsch = $I:\{\bar{2}\bar{1}2\}$ Palache
Λ $\{\bar{1}02\}$ Heritsch = $\Lambda:\{102\}$ Palache
Ξ $\{302\}$ Heritsch = Ξ $\{\bar{3}02\}$ Palache

Heritsch also accepts two previously reported forms which are not mentioned by Palache. Neither of these seems sufficiently well sup-

[1] Take the axis of the main zone as [001]. Let (001) slope front-right. Make [010] longer than [100].

ported to be included in the list of accepted forms; they may be retained as uncertain, subject to confirmation.

s{$\bar{1}73$} Flink (1916), setting of Dana (1892) = {$3\bar{1}3$} Palache. Such confusion surrounds the indices of this form (Heritsch, 1937, p. 264) that it is better regarded as uncertain.

x{$\bar{3}13$} Lodočnikow (1927), setting of Schrauf (1870) = {$\bar{1}32$} Palache. Determined once with the microscope on a minute grain.

Lattice Dimensions

The lattice dimensions of axinite given by Schiebold (1931, p. 311, footnote 36) are based on previously unpublished measurements by Schiebold and Eulitz on a crystal from Bourg d'Oisans. The method of measurement and limits of error are not stated. Replacing Schiebold and Eulitz's original value for the axial angle γ by its supplement and transforming the elements according to the formula already given we have

	Schiebold & Eulitz (1931)		Peacock (1937)
	Original	Transformed	
a_0	8.966Å	7.020Å	7.151Å
b_0	9.017Å	9.017Å	9.184Å
c_0	7.020Å	8.966Å	8.935Å
α	102°38′	91°49′	91°52′
β	82°01′	97°59′	98°09′
γ	88°11′ [91°49′]	77°22′	77°19′

the satisfactory comparison given above. The writer's values were obtained from Weissenberg photographs about each of the three principal lattice axes, giving accurate duplicate values for the spacings of the axial planes and precise values, independent of the external geometry, for the reciprocal axial angles.

Twinning

In stating that axinite is free from twinning (1937, p. 591) the writer was unaware of a paper by Lodočnikow (1927) who described twinning in a single grain of axinite (0.1 mm.^{2}) in a rock section, on the basis of observations with the microscope and universal stage. In Schrauf's notation Lodočnikow determined the composition plane of the intergrowth as (110) and the twin axis as the edge (110)/($\bar{3}13$) = [$3\bar{3}4$]. In our notation the twin law would be: twin axis [023]; composition plane (100).

While admiring the skill with which this observation was made and the ingenuity of the argument leading to the symbol ($\bar{3}13$), which is fur-

ther advanced as the new form χ, we feel that Dr. Lodočnikow's twin law requires confirmation on goniometrically measurable crystals.

Summary

To an earlier account of the crystallography of axinite (1937) the following may be added. Symmetry: pedial rather than pinakoidal. Forms: $K:\{3\bar{2}0\}$, $I:\{\bar{2}\bar{1}2\}$, $\Lambda:\{102\}$, $\Xi\{\bar{3}02\}$ (Heritsch, 1937); uncertain: $\{\bar{3}\bar{1}3\}$ (Flink, 1916), $\{\bar{1}\bar{3}2\}$ (Lodočnikow, 1927). Twinning (requires confirmation): twin axis [023], composition plane (100) (Lodočnikow, 1927).

Three previously overlooked settings of axinite are given: Fedorov (1901), Fedorov (1920), Schiebold (1931). Palache's geometrical elements are confirmed by new measurements (Heritsch, 1937). Previously unnoticed lattice dimensions (Schiebold and Eulitz, 1931) are in essential agreement with Peacock's structural elements.

References

Dana, E. S. (1892): *System of Mineralogy*, ed. 6—New York.

Donnay, J. D. H. (1937): Transformation of co-ordinates—*Am. Mineral.*, vol. **22,** pp. 621–624.

Fedorov, E. S. (1901): *Textbook of Crystallography*, ed. 3—St. Petersburg.

——— unter Mitwirkung von D. Artemiew, Th. Barker, B. Orelkin und W. Sokolow (1920): Das Krystallreich—*Mem. Russ. Ac. Sci.*, ser. 8, vol. **36,** pp. 1–1050+212.

Flink, G. (1916): Bidrag till Sveriges mineralogie—*Ark. Kemi*, vol. **6** (21), pp. 1–149.

Ciebe, E., and Scheibe, A. (1925): Eine einfache Methode zum qualitativen Nachweis der Piezoelektrizität von Kristallen—*Zeits. Physik*, vol. **33,** pp. 760–766.

Goldschmidt, V. (1897): *Krystallographische Winkeltabellen*—Berlin.

Heritsch, H. (1937): Ein Beitrag zur Morphologie des Axinits—*Zeits. Krist.*, A, vol. **96,** pp. 249–272; 337–356.

Hintze, C. (1897): *Handbuch der Mineralogie*, vol. **2**—Leipzig.

Lodočnikow, W. N. (1927): Ein Zwilling und eine neue Axinitfläche im Albitophyr des Tarbagatai—*Zeits. Krist.*, vol. **65,** pp. 122–133.

Martin, A. J. P. (1931): On a new method of detecting pyroelectricity—*Min. Mag.*, vol. **22,** pp. 519–523.

Peacock, M. A. (1937): On the crystallography of axinite and the normal setting of triclinic crystals—*Am. Mineral.*, vol. **22,** pp. 588–620.

Schiebold, E. (1931): Über die Isomorphie der Feldspatmineralien—*N. Jb. Min.*, Beil. Bd. **64A,** pp. 251–319.

Schrauf, A. (1870): Mineralogische Beobachtungen, I—*Sitzungsber. Akad. Wiss., Wien*, vol. **62** (2), pp. 699–760.

YEATMANITE, A NEW MINERAL, AND SARKINITE FROM FRANKLIN, NEW JERSEY

CHARLES PALACHE, *Harvard University*, L. H. BAUER, *Franklin, N. J.*, AND HARRY BERMAN, *Harvard University.*

ABSTRACT

Yeatmanite, $(Mn, Zn)_{16}Sb_2Si_4O_{29}$, is a new mineral from Franklin, N.J. It is triclinic, pseudo-orthorhombic, with multiple twinning on $b(010)$ and macroscopic twinning on (023). Elements (x-ray): $a:b:c=0.7811:1:0.4775$. $\alpha=103°49'$; $\beta=101°45'$; $\gamma=87°12'$. Cleavage perfect $\|(100)$; H. 4, G. $5.02\pm.10$. Biaxial, negative; X near $a[100]$, Y near $b[010]$, $Z\wedge c[001]=3\frac{1}{2}°$. Indices (Na): nX $=1.873$, nY $=1.905$, nZ $=1.910$, all ±0.003. 2V about 49°, r < v, dispersion moderate. Clove-brown crystalline plates embedded in willemite. The composition of sarkinite, associated with the yeatmanite, differs from the Långban material only in having 5.38 per cent of zinc.

In the spring of 1937 a few specimens were found in the mine at Franklin, in which an unfamiliar pink mineral attracted attention. Mr. Bauer examined this mineral and made micro-chemical tests which revealed the presence of arsenic, manganese and zinc. Optical tests showed the characters of sarkinite, a mineral found before only at Långban and Pajsberg in Sweden. The sarkinite is embedded in green willemite, the two forming together a narrow vein in massive granular ore. In the willemite is a very small amount of an additional mineral in the form of clove-brown plates, which proves to be a new species. It is described in the following pages and to it has been given the name yeatmanite, in honor of Pope Yeatman, the distinguished mining engineer, who has been closely associated during recent years with mining and milling operations at Franklin.

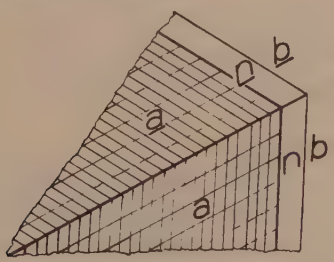

FIG. 1. Yeatmanite crystal twinned on (023).

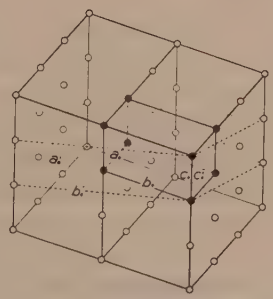

FIG. 2. Yeatmanite lattice.

Yeatmanite. The plates of yeatmanite are embedded in willemite and reach a maximum dimension of 1.3×0.7 cm. with a thickness of 1 mm.

Generally irregular in outline or lath-shaped, one or two were found with pseudohexagonal crystal form as shown in Fig. 1. This is clearly a twin crystal and was at first taken to be composed of orthorhombic individuals. Optical examination, however, proved that the striae shown on the broad face are due to lamellar twinning on $\{010\}$ and that the individual is really triclinic. The few angles measured are insufficient to define the elements of the crystal, which was, however, analyzed by x-ray data as shown below. The tabular face of the plates was taken as $\{100\}$ and the direction of twinning striae on that face as the vertical. The measurements obtained are as follows:

$a(100) \wedge b(010) = 90°00'$ circa
$a(100) \wedge n(210) = 20°00'$ circa
$b(010) \wedge n(210) = 60°00'$

The x-ray study was made on one member of such a twin as is shown in Fig. 1. Weissenberg photographs were made of the equatorial and first layers, with $c[001]$ as rotation axis. The first layer line shows a symmetry plane $\{010\}$ corresponding with the twin plane of the lamellae determined by optical examination of the same crystal. No other plane of symmetry could be detected in the x-ray photograph. This evidence, together with the optical data, leads to the conclusion that yeatmanite is triclinic. Calculation of the simplest triclinic cell yields:

$a_0 = 9.029$, $b_0 = 11.56$, $c_0 = 5.52$ all $\pm .01$Å. $\alpha = 103°49'$, $\beta = 101°45'$, $\gamma = 87°12'$ (The angles are probably not more accurate than $\pm 1°$.)

Crystallographic elements calculated from these values are: $a:b:c = 0.7811:1:0.4775$; $\alpha = 103°49'$, $\beta = 101°45'$, $\gamma = 87°12'$; $p_0' = 0.6245$, $q_0' = 0.4918$, $x_0' = 0.2080$, $y_0' = 0.2461$, $\lambda = 76°27'$, $\mu = 78°35'$, $\nu = 90°00'$.

Forms: $a\{100\}$, $b\{010\}$, $n\{210\}$, $\{023\}$—the last observed only as a twin plane.

A pseudo-orthorhombic cell containing six triclinic units has the attitude shown in Fig. 2 and the dimensions a_0'26.53, b_0'22.43, c_0'5.52Å. This multiple cell is also produced by twinning on $\{010\}$ and this identity probably accounts for the twin structure.

Optical properties. The crystal used for the x-ray study was also used for optical examination. The acute negative bisectrix is apparently normal to the $a\{100\}$ face and the plane of the optic axes is inclined $3\frac{1}{2}°$ to the trace of the twin plane $b\{010\}$ as seen on $a\{100\}$. Refractive indices measured with phosphorus methylene iodide liquids are as follows: $n\mathrm{X} = 1.873$, $n\mathrm{Y} = 1.905$, $n\mathrm{Z} = 1.910$, all $\pm .003$ for sodium light. The dispersion is moderate $r < v$ and the axial angle is about 40° as estimated. (From the indices of refraction $2\mathrm{V} = 49°$.) No pleochroism was noted.

Physical properties. Yeatmanite has an excellent cleavage on $a\{100\}$.

It is brittle. The color is deep brown in the larger pieces and light brown in thin fragments. The streak is very light brown. Hardness is 4. The density as determined by H. Winchell on a sample of .073 gm., using a micropycnometer, is 5.02 ± 0.10. This sample contained some willemite and a small percentage of calcite.

Chemistry. A sample of yeatmanite of about 0.45 gram was prepared and analyzed. Its composition and ratios are presented in the first table. A second specimen was found by Mr. Bauer in his collection, of unknown origin. From this a sample of about 0.7 gram was prepared and yielded the figures of Table 2.

YEATMANITE—Sample 1

	1	2	3		4	
SiO_2	13.50	13.59	.226	$= 4\times.057$	Si	3.8
Sb_2O_5	18.01	18.12	.056	$= 1\times.056$	Sb	1.9
MnO	33.00	33.21	.469			
FeO	0.36	0.36	.005	$.901 = 16\times.056$	R	15.0
ZnO	34.54	34.72	.427			
H_2O+	0.54	—				
	99.95	100.00				

1. Analysis of 0.45 gram (used in 3 portions). L. H. Bauer, *analyst.*
2. Corrected for water.
3. Molecular proportions.
4. Atoms in unit cell.

YEATMANITE—Sample 2 (treated with dilute HCl)

	1	2	3		4
SiO_2	14.16	14.31	.238	$= 4\times.060$	13.48
Sb_2O_5	18.48	18.68	.058	$= 1\times.058$	18.15
MnO	37.06	37.45	.535		36.53
FeO	0.90	0.91	.013	$.987 = 16\times.062$	
ZnO	28.35	28.65	.439		31.84
H_2O+	0.45	—			
CaO	present	—			
	99.40	100.00			100.00

1. Analysis of 0.7 gram (used in 3 portions). L. H. Bauer, *analyst.*
2. Corrected for water.
3. Molecular proportions.
4. Theoretical composition for $(Mn, Zn)_{16}Sb_2Si_4O_{29}$ with Mn:Zn 1:1.

Both analyses yield substantially the same formula, which is $(Mn,Zn)_{16}Sb_2Si_4O_{29}$, with about equal molecular parts of Mn and Zn.

The number of atoms in the unit cell is given in column 4 of the first table, calculated from the volume and density. These values are about 6% too low, and the calculated density, 5.37, differs from the found value

by about that amount. This maximum error is the result of cumulative error in three independent sets of data.

Tests. Yeatmanite fuses at about 4 to a black slag. It is easily soluble in dilute HCl. To show the presence of antimony use the following micro test. Dissolve a grain of yeatmanite in a drop of HCl, 1:1. Warm slowly, then add several drops of water and a drop of KI solution, the latter to reduce $SbCl_5$. Then with a capillary tube touch the solution with H_2S gas and note characteristic orange precipitate of Sb_2S_3.

Yeatmanite shows no clear relation to any previously described antimoniosilicate. It is the first mineral to be found at Franklin containing antimony. Its discovery, as well as that of sarkinite, adds two more features of resemblance between the mineral assemblages of Franklin and Långban.

Sarkinite. The pink mineral with which yeatmanite occurs shows no crystals. It is of a lively pinkish red color and shows a trace of cleavage in one direction. The optical properties are: Biaxial, negative; $r<v$. Indices: nX = 1.790, nY = 1.794, nZ = 1.798, all $\pm$.003.

The chemical analysis yields a formula in good agreement with type material of sarkinite, which, however, contains no zinc.

Analysis of Sarkinite, L. H. Bauer, *analyst*

As_2O_5	40.73
SiO_2	0.14
MnO	48.09
ZnO	5.38
FeO	0.18
CaO	0.20
MgO	0.67
Cl	0.05
H_2O (+110°C)	3.22
	98.66

We desire to express our thanks to the officials of the New Jersey Zinc Company for permission to use the chemical data for publication.

A SUBSTITUTE FOR THE QUARTZ WEDGE USED WITH THE POLARIZING MICROSCOPE

C. D. West, *The Land-Wheelwright Laboratories, Inc., Boston, Mass.*

The ungraduated quartz wedge has long been used with the polarizing microscope for two types of purposes: (1) to determine the directions of fast and slow rays and to measure roughly by compensation the retardation of a flat birefringent section in parallel white light; (2) to find the character of birefringence, or differentiate the fast and slow rays in a birefringent section by other methods than simple compensation in parallel white light. Under the second heading come several different methods, such as finding the sign of birefringence in convergent white or colored light from the motion of the isochromatic bands; finding the fast and slow rays in a wedge-shaped section in parallel light (white or colored) from a similar motion of the isochromatic bands; and finding the fast and slow rays in a thick section in parallel white light by the motion of dark interference bands across the spectrum, according to the method recently described by Lietz (1937). The methods of this second class are often used when the section under examination has a high retardation or when it is strongly colored. The quartz wedge is used often enough in these several ways to make it a standard accessory in petrographic work, in spite of its high cost ($25 from American dealers) as compared with other compensator plates.

One substitute for the quartz wedge is found in the step plate known as Fedorov's comparator or mica echelon (Johannsen (1918)), or the earlier step plate described in the English literature as the Fox Wedge. Such plates, if they can be obtained, cost about as much as the quartz wedge.

A combination of quarter-wave plate and rotating analyzer has long been used by physicists for the analysis of elliptically polarized light by Mach's method (Rinne-Berek (1934)). This combination was adapted by Senarmont and by Friedel for the purpose of measuring retardations with the polarizing microscope, and is occasionally mentioned in the literature (Ambronn-Frey (1926); Wright (1911)). Wright's statement that the method has not been generally adopted by petrologists is as true today as it was when it was written.

Strangely enough, the use of the same combination of quarter-wave plate and rotating analyzer for the second class of purposes mentioned above seems to be nowhere referred to in the literature of the polarizing

microscope. For such purposes it is shown in the following that the combination is a practical substitute for the quartz wedge, and at a cost of less than half that of the latter.

For such purposes the specimen is oriented as usual in the diagonal position with respect to the polarizer, and a quarter-wave plate is inserted above the specimen with one of its vibration directions parallel to the vibration direction of the polarizer. On now rotating the analyzer, the isochromatic bands (or dark interference bands in Lietz' method) move in or out in exactly the same manner as when a quartz wedge is used, and from the sense of their motion exactly the same inferences may be drawn concerning the shape or orientation of the index-ellipsoid of the specimen.

Concerning the sense of the motion it is immaterial whether the vibration direction of the polarizer is horizontal or vertical. If the slow ray of the quarter-wave plate is horizontal (left-to-right) and the analyzer is rotated in a clockwise direction, then the motion of the isochromats or interference bands is the same as that given by a conventional quartz wedge (Fig. 1). (The same statement is true if the analyzer is fixed, the quarter-wave plate is inserted with its slow ray horizontal below the specimen, and the polarizer is rotated in a clockwise direction). The question can of course be decided by trial with a piece of mica or other suitable known crystal. A 180° rotation of the analyzer in the one case is equivalent to a translation of the wedge from a point of retardation x to a point of retardation $x+\lambda$ in the other case.

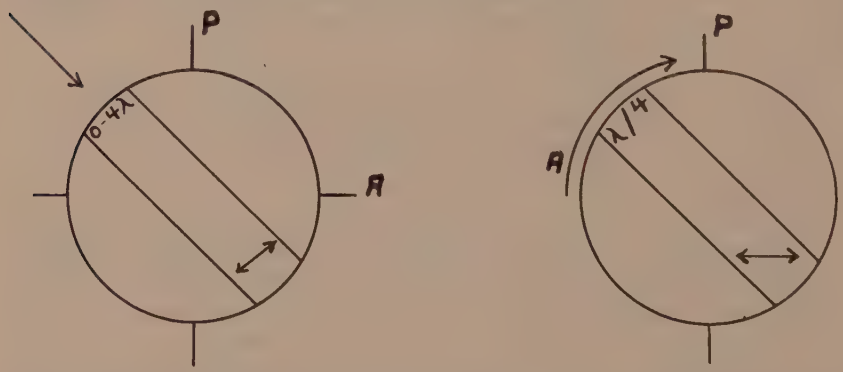

FIG. 1

Quartz wedge inserted in direction of arrow. Slow ray and thin edge marked by ⟷.

Analyzer rotated in direction of arrow. Slow ray of λ/4 plate marked by ⟷.

It is often of advantage to make the isochromatic bands more distinct by using light filters or monochromatic light. For the present purposes

if the quarter-wave plate used is for the middle of the visible spectrum (retardation 137 to 147 millimicrons) it will give satisfactory results for any wavelength or band of the visible spectrum.

If the combination described is used with a standard polarizing microscope (diagonal compensator slot) a special quarter-wave plate must be obtained with the orientation shown in the figure, since in ordinary compensation plates the vibration directions are parallel to the edges of the fitting.[1]

References

Ambronn H. and Frey, A. Das Polarisationsmikroskop. *Leipzig*, **1926,** p. 63.
Johannsen, A. Manual of Petrographic Methods. *New York*, **1918,** p. 379.
Lietz, J. *Zeits. Krist.*, vol. **97,** p. 122, 1937.
Rinne F. and Berek, M. Untersuchungen mit dem Polarisationsmikroskop. *Leipzig*, **1934,** p. 223.
Wright, F. E. Methods of Petrographic-Microscopic Research. *Washington*, **1911,** p. 103.

[1] A cap analyzer ($7.50) and cap quarter-wave plate ($4.50) are listed under their "Polaroid Micro Accessories" by the Bausch & Lomb Optical Company; these fit over any ocular up to 27 mm. in diameter and are suitable for the present purposes if a pin in the quarter-wave plate mounting is removed so that the analyzer can be rotated freely.

NOTES AND NEWS

ZONING AS AN EXPLANATION OF OPTICAL ANOMALIES OF A PLAGIOCLASE FELDSPAR IN QUARTZ-BEARING PLUTONITES FROM VERMONT

MALCOLM M. MULHOLLAND,
Syracuse University, Syracuse, New York.

The "granites" of Vermont have long been famous as a source of monumental stone. In 1909, Dale[1] of the U. S. Geological Survey, made the most extensive study of these rocks that has been made to date, although he states it was not "an exhaustive geologic and petrographic account of the Vermont granites."

In 1934, Maynard[2] restudied some of these rocks and arrived at conclusions which differed considerably from those of Dale. Whereas Dale had reported orthoclase in many of these plutonites, Maynard found orthoclase in only two of the eight specimens that he studied. From his work on the "Bethel white granite" he found that "Oligoclase of the composition *Ab* 82 *An* 18, instead of quartz, as stated by Dale, is the most abundant constituent . . . . Orthoclase was not found in the thin section studied or in any of the numerous samples that were crushed and examined in oils. It is probable that Dale mistook some of the oligoclase for orthoclase as much of it does not show albite twinning, and quite often does show Carlsbad twinning."

Maynard's study led him to conclude that because of the abundance of plagioclase feldspar in these rocks, the paucity of twinning on the albite law, and the almost complete absence of orthoclase, it might be of value to study the plagioclase in detail to see if its optical and chemical properties corresponded with those given in the literature. This paper deals mainly with the optical phase of this problem.

The three specimens used in this study were collected (1) from the Newport Granite Company's quarry, near the center of the town of Derby; (2) along the road connecting Greensboro and East Craftsbury, just north of the town of Greensboro; and (3) from the Woodbury Granite Company's quarry on Robeson Mountain, east of the town of Woodbury.

The plagioclase which occurs in these rocks is unique in that the majority of the grains do not show albite twinning. Some however do show a patch of albite twinning near the center of the grain, or more rarely are completely twinned according to this law. Occasionally twin-

[1] Dale, T. N., The granites of Vermont, *U. S. Geol. Survey*, Bull. **404**, 1909.

[2] Maynard, James E., The re-examination of quartz-bearing plutonites from Vermont: *Jour. Geol.*, vol. **42**, no. 2, 1934.

ning according to the Carlsbad law, and a combination of Carlsbad and albite twinning is present. Much of the feldspar shows pronounced zoning. Inclusions of sphene, apatite, and possibly zircon, are present in varying amounts. Alteration products of the feldspar are kaolin, muscovite, calcite and epidote.

The refractive indices were determined for each specimen by the immersion method using monochromatic light. This procedure served to outline the limits of the zoning and gave some idea as to the average composition. With the exception of the Greensboro specimen the limits ranged between *Ab* 76 and *Ab* 84.

The extinction angles were measured between the fast ray and traces of the {010} and {001} cleavages. The compositional limits indicated by these angles all fall within one per cent of a range of *Ab* 74 to *Ab* 87, a greater variation than is shown by the refractive indices, which are no doubt more accurate. The average composition of the plagioclase, computed for all specimens, from the refractive indices and extinction angles, varies between *Ab* 80 and *Ab* 81.

A total of ten optic signs was determined for each specimen from good optic axis figures, and from six to ten of these were positive in each case. Since a positive optic sign indicates a composition varying between *Ab* 84 and *Ab* 100, the high percentage of positive signs is anomalous with respect to the composition indicated by the other optical properties, which show that a composition of *Ab* 84 is near the extreme acid limit of the zoning.

No reason for this apparent anomaly was suggested until the zoning of the plagioclase was examined in some detail. This study showed that in the majority of the grains the zoning was of the reverse type, having sodic cores and becoming progressively more calcic toward the borders. This type of zoning is relatively rare and has never been reported for these rocks. Larsen[3] and his associates have recently noted its occurrence in the plagioclase of the San Juan lavas.

It seems logical to conclude that zoning of this type would yield a greater number of positive optic signs than negative, in spite of the fact that the average composition was more basic than *Ab* 84. A grain having a sodic core could have a thin zone of calcic feldspar at the outer border which would more than equal the volume of the inner zones. The optic sign would be determined by the more compact sodic core, whereas the composition of the grain as a whole would be more calcic than indicated, due to the more calcic outer zones. Grains which in sectioning had been

[3] Larsen, E. S., and others, Petrographic results of a study of the minerals from the Tertiary volcanic rocks of the San Juan region, Colorado: *Am. Mineral.*, vol. **23**, pp. 230–231, 1938.

cut through and parallel to one of the calcic zones would properly show a negative sign, but these would be less frequent than grains showing a positive sign.

It will be necessary to make a chemical analysis of the plagioclase in each rock to conclusively establish its actual composition. The first of these analyses has been made for the Derby rock and the results are:

SiO_2	60.83
Al_2O_3	22.22
Fe_2O_3	0.93
TiO_2 & ZrO_2	1.07
MgO	0.40
CaO	4.84
Na_2O	8.44
K_2O	0.62
H_2O	0.90
	100.25

The composition in weight per cent, calculated from the analysis to 100% is:

Orthoclase	4%
Albite	72%
Anorthite	24%

Since nearly all the standard tables in the literature treat plagioclase as a two component series, it seems justifiable to include the orthoclase with the albite, giving a composition of *Ab* 76 *An* 24 for this feldspar. This single analysis does not carry much weight, but it indicates that the anomaly between certain of the optical properties, as a result of reverse zoning, is more important than seems apparent from optical data alone.

LOSS OF NICKEL FROM METEORITES THROUGH WEATHERING

H. H. Nininger, *Colorado Museum of Natural History, Denver, Colorado.*

The failure of meteorites to appear in any of the pre-glacial formations has long been a puzzle to geologists as well as to students of meteorites. Suggestions relative to the recognition of meteorites have usually been based on the assumption that the nickel content should be regarded as the best indication of meteoritic origin. In 1929 the writer pointed out that in oxidized specimens from Brenham, Kiowa County, Kansas, the nickel content had shrunken proportionately far more than had the iron content from the original composition as determined on well-preserved specimens of the same fall.

Recently we have gained additional light on the loss of nickel from oxidized meteorites. This new information was obtained experimentally in the following manner: one of the oxidized meteorites which had been removed during our excavation of the Haviland meteorite crater was used in this experiment. The specimen which weighed 211 grams was broken up into chunks averaging about the size of marbles. These fragments were immersed in tap water and allowed to stand for two hours, being shaken several times during this period. After this treatment some dimethylglyoxime was added. A heavy precipitate of Ni-glyoxime appeared. A 30 cc. sample of this same solution was reserved for quantitative analysis. This was submitted to the firm of Wilfley and Bribach, chemists of Denver, Colorado, for a nickel determination. Duplicate determinations were made showing nickel to be present at the rate of .08532 grams per liter of the solution. The same fragments were then rinsed through several baths of water and allowed to stand in 600 cc. of fresh tap water for ninety-five days, after which a 60 cc. sample was submitted to the same chemists for analysis. The tests were run in duplicate and this time the yield of nickel was at the rate of .07299 grams per liter. Both the chloride and the sulphate acid radicals were found to be present in the solution.

The metallic portion of well-preserved specimens of this pallasite from Kiowa County, Kansas, was analyzed years ago. For these tests the bright untarnished metal was used. Two of the results are given below:

	Fe	Ni
L. G. Eakins	88.4 %	10.35%
Winchell & Dodge	90.48%	8.59%

The specimen used in our recent experiments was so completely oxidized that none of the original metal remained. (As explained in our report on the excavation of the Haviland meteorite crater, these crater specimens had succumbed to the forces of weathering due to their greater exposure. See *Proc. Colo. Mus. Nat'l. Hist.*, vol. 12, No. 3.) The metallic portion had been altered to limonite, principally. A sample of this limonitic material was found to contain 1.47% nickel. It is therefore evident that the nickel content had been materially reduced during the years since the arrival of the meteorite (date of fall unknown). It is also evident that the loss of nickel is still going on.

It is the writer's belief that an exhaustive study of this process of the leaching of nickel would yield important information relative to the age of some meteorites that have been recognized and that it might also eventually enable us to identify meteorites heretofore unrecognizable in the older rocks.

BOOK REVIEWS

MINERAL TABLES by Arthur S. Eakle; third edition, revised by Adolf Pabst. 73 pages. John Wiley & Sons, Inc., *New York*, **1938.** Price $1.50.

These well known tables for the determination of minerals by their physical properties follow the style and arrangement of the earlier editions. Minor changes have been made and a number of additional species included so that the tables in their present form contain descriptions of about two hundred minerals.

W. F. H.

MINERALS OF CALIFORNIA by Adolf Pabst. Bulletin No. **113,** State Division of Mines, Ferry Building, *San Francisco*, California, 1938.

This is a revision of Bulletin No. **91** bearing the same title and issued in 1923. All of the older references on the occurrence of minerals in California have been checked and the list extended so that the present bulletin contains descriptions and occurrences of over four hundred different minerals, forty-one of which have not thus far been found elsewhere. The bulletin concludes with a bibliography of twenty-one pages arranged alphabetically by authors.

W. F. H.

MINERALOGIE VON BOLIVIEN by Friedrich Ahlfeld and Jorge Muñoz Reyes. Gebrüder Borntraeger, *Berlin*, **1938.** 89 pages. Price RM 10.50.

This pamphlet is a German translation of a somewhat more extended work by the same authors in Spanish (Mineralogia Boliviana). Here are recorded the descriptions (crystallographic and chemical) and occurrences of 171 mineral species, based largely on the studies of the senior author which have extended over a long period. A special effort has been made to include wherever possible a discussion involving petrogenesis. Stress has been placed on cassiterite and associated minerals while the common rock-forming minerals are given but slight consideration. The text contains 30 crystal drawings of simple and twinned crystals and the bibliography records 75 references. This German translation makes accessible to all mineralogists and mining engineers information concerning the mineral wealth of this interesting country.

W. F. H.

PROCEEDINGS OF SOCIETIES

MINERALOGICAL SOCIETY OF GREAT BRITAIN AND IRELAND

June 10, 1938

Dr. L. J. Spencer, President, in the Chair. The following papers were read:

(1) *The leaching of granite and other rocks.* By Mr. E. H. Davison.

The paper describes experiments devised to determine the solubility of granite and other rocks in aerated, distilled water. The water is allowed to drip through the crushed rock and is afterwards evaporated and the residue of dissolved material weighed. The accumulated solubles after 25 leachings are analysed. The results show definite solubility in granite, gabbro, and oolitic limestone.

(2) *Some new and little-known meteorites found in Western Australia.* By Dr. E. S. Simpson.

Accounts are given of 14 meteorites (11 siderites, 2 stones, and one seen to fall but not yet found), of which 8 are new, bringing the total number known from Western Australia up to 23. New are Dalgaranga (siderite), Dowerin (siderite), Gundaring (siderite, 248 lb.,

fell April 6th, 1930, found 1937), Kumerina (siderite, 118 lb., found 1937), Landor (siderite), Mellenbye (stone), Wonyulgunna (siderite, 83½ lb., found 1937), and Yalgoo (stone). Meteorites previously described under the names Youndegin, Mount Stirling, and Mooranoppin are identical in structure and chemical composition, and they have all been found on an area of some ten square miles close to Pikaring (Penkarring) Rock, 34 miles S.E. of Youndegin.

(3) *Francolite from sedimentary ironstones of the coal measures.* By Mr. T. DEANS, with a chemical analysis by Mr. H. C. G. VINCENT.

Francolite occurs in oolitic ironstones from the Yorkshire coalfield as small hexagonal plates showing twinning in six sectors. The optical properties, including anomalous features found in other members of the apatite group, are described. Analysis establishes the formula $(Ca, Sr)_{10}(P, C)_6(F, OH)_2O_{24}$.

(4) *On the atomic arrangement and variability of the members of the montmorillonite group.* By Dr. G. NAGELSCHMIDT.

X-ray data for the montmorillonite group are given and discussed. The group is shown to have three end-members, Al_2R (montmorillonite) Fe_2R (nontronite) and Mg_3R (magnesium-beidellite) where R is possibly Si_4O_{10} $(OH)_2$. The number of hydroxyls is not quite certain.

Calculations based on the assumption of a three-layer lattice for these minerals show fairly large isomorphous replacements, which are believed to be essential, and a balance between the negative charges due to the replacements and the exchangeable excess cations. The need for more detailed information on these minerals, especially with regard to their dehydration curves, is pointed out.

(5) *On chamosite and daphnite.* By Dr. A. F. HALLIMOND.

Relatively pure chamosite found in a Cardinia shell in the Frodingham Ironstone has the simple ratio $2SiO_2 \cdot Al_2O_3 \cdot 3FeO \cdot nH_2O$. Daphnite from Tolgus Mine differs somewhat from this ratio, belonging to a series extending toward the ordinary chlorites. Neither mineral is represented by the Tschermak formula. *X*-ray photographs of chamosite are constant in pattern and closely resemble those of cronstedtite. Daphnite and thuringite give patterns nearly identical with those of clinochlore but the spacings are slightly different. The two minerals studied are distinct varieties of chlorite. Chemical analyses are by Mr. C. O. Harvey and *x*-ray measurements by Mr. F. A. Bannister.

(6) *The identity of zinckenite and keeleyite.* By Mr. G. VAUX and Mr. F. A. BANNISTER.

Zinckenite from Wolfsberg, Harz, and keeleyite from Oruro, Bolivia, were compared by means of single crystal *x*-ray photographs about the *c* axis, and were found to be identical. No twinning was discovered in zinckenite which was found to be truly hexagonal with $a=44.06$, $c=8.60$Å, space-group $C_6^6=C6_3$ or $C_6^2=C6_3/m$.

(7) *A chemical and optical study of a low-grade actinolitic amphibole from Coronet Peak, Western Otago, New Zealand.* By Mr. C. OSBORNE HUTTON.

The chemical analysis and optical constants of an actinolitic amphibole from a low-grade albite-epidote-actinolite-chlorite-calcite schist are given. It is shown that the maximum ext. angle in the prism-pinacoid zone is not to be obtained on a clinopinacoidal section. Details of a rare amphibole comparable with crossite in its optical properties are also given.

(8) *An x-ray examination of mordenite (ptilolite).* By Messrs. C. WAYMOUTH, P. C. THORNLEY, and W. H. TAYLOR.

Specimens of the fibrous zeolite mordenite (ptilolite) have been examined by x-ray methods, and the specific gravity and pyroelectric properties determined. Laue- and oscillation-photographs indicate that the structure possesses orthorhombic symmetry, and the unit cell with axes: $a=18.25$Å., $b=20.35$Å., $c=7.50$Å., contains four molecules of composition $(Ca, K_2, Na_2)Al_2Si_{10}O_{24}\cdot 7H_2O$. The space group is $D_{2h}^{17}-Cmcm$ or $C_{2v}^{12}-Cmc$; the pyroelectric tests are somewhat inconclusive but indicate that the c-axis [001] is probably polar. The structure is probably based on a frame-work of linked tetrahedra.

PHILADELPHIA MINERALOGICAL SOCIETY

Academy of Natural Sciences of Philadelphia, April 7, 1938

A stated meeting was held on the above date with the president, Mr. Trudell, in the Chair, 43 members and 26 visitors were present.

The speaker of the evening was Mr. Richmond E. Myers, whose subject was "Collecting Minerals in the U.S.S.R." Mr. Myers attended the 17th International Geological Congress, taking the excursion through the Caucasus Mountains and Armenia, to the Persian border. The speaker said there was little opportunity for collecting at the localities visited, however, specimens were set aside. Mr. Myers visited the Moscow Museum where he was treated with great courtesy. Motion pictures of the cities and localities visited were shown and specimens obtained on the trip exhibited.

LOUIS MOYD, *Secretary*

Academy of Natural Sciences of Philadelphia, May 5, 1938

A stated meeting was held with the president, Mr. Trudell in the Chair, 51 members and 33 visitors were present.

Dr. Benjamin L. Miller of Lehigh University, spoke on "Experiences in Russia, Korea, China and Japan." Dr. Miller attended the Geological Congress in Russia last summer, taking the excursions through the Caucasus and Urals, and then traveling on through Asia. He described many of the mining localities visited. The Urals are eroded pre-Cambrian rocks. These rocks are the source of the metals now being dredged from the alluvial gravels, especially platinum. At one place a mine is being operated for iron from a pisolitic laterite which caps a highly altered and weathered ultrabasic dike. This deposit is similar to those worked in Cuba.

In Manchuria Dr. Miller visited a coal mine with a bed of coal 400 feet thick, containing an unusual quantity of amber, some of which includes insects. Overlying the coal seam is a bed of oil shale from which kerosene is obtained, and a bed of calcareous shale that is being burned for lime; altogether a very profitable deposit.

In Japan, on a small island 10 miles from Nagasaki, the speaker descended a 2000 foot shaft into a coal mine which is being worked by drifting out beneath the sea. The presence of the coal bed at that depth was determined by tracing the dip where the bed outcropped on a neighboring island. Dr. Miller visited the great caldera of Mt. Osso, which measures 10×14 miles and contains 11 villages. Sixty-eight small craters are found on the floor of the caldera and sulfur is being mined from some of the active vents. The sulfur is deposited in the porous volcanic rock by the vapors. The lecture was illustrated with many interesting slides.

LOUIS MOYD, *Secretary*

Academy of Natural Sciences of Philadelphia, June 2, 1938

A stated meeting was held with the president Mr. Trudell in the Chair, 51 members and 31 visitors were in attendance.

Mr. A. Williams Postel of the University of Pennsylvania spoke on his study of the granite gneisses of the Chester Quadrangle. The speaker found xenoliths showing all stages of reaction with the granite. These xenoliths, he believes, are remnants of the amphibolite facies of the Wissahickon gneiss. Unaltered cores of some of the xenoliths resemble normal amphibolites, but the rocks become more acidic as the granite is approached. The labradorite of the amphibolite is changed to andesine, then to a sodic oligoclase. The hornblende alters to biotite, with epidote forming from the lime released by these changes. In the contact zone a very unusual symplektite becomes an important constituent of the rock.

Mr. Joseph Berman described this symplektite as an intergrowth of magnesium muscovite (phengite) and oligoclase. Its origin, he believes, is due to reaction between biotite and basic plagioclase in the presence of acid solutions.

Dr. Joseph L. Gillson described some unusual varieties of fluorite from the localities he had visited during the past few months: among these were a chalky, white type of extreme purity, and stalactitic and botryoidal types from Nevada and Utah. Other members displayed numerous specimens collected on trips recently taken.

LOUIS MOYD, *Secretary*

An organization meeting of the Plainfield Mineralogical Society was held at the home of Mr. Thomas A. Wright, Tuesday evening June 7, 1938. Thirteen persons were present and others unable to attend expressed their desire to join. Present plans call for monthly meetings from October to May with field trips scheduled to be held during the summer months. The first field trip to Bedford, New York, was taken on June 19. The officers for the ensuing year are: Honorary President, Alfred C. Hawkins; President, Thomas A. Wright; Secretary-Treasurer, Joseph D'Agostino; Chief Scout, O. Ivan Lee.

NEW MINERAL NAMES

Skolite

KAZIMIERZ SMULIKOWSKI: Skolite, a new mineral of the glauconite group. *Arch. Mineral. Warsaw*, vol. **12**, pp. 144–180, 1936. French; Polish summary.

NAME: From the village Skole, Poland, where the mineral was first found.

CHEMICAL PROPERTIES: A hydrous silicate, related to glauconite: $H_4K(MgFe'', Ca)(Al, Fe''')_3Si_6O_{20} \cdot 4H_2O$. Analysis: SiO_2 49.09, Al_2O_3 18.17, Fe_2O_3 6.42, FeO 2.56, MgO 3.10, CaO 1.03, K_2O 5.62, Na_2O 0.23, H_2O 13.47, TiO_2 0.21, P_2O_5, MnO tr. Sum 99.90.

PHYSICAL AND OPTICAL PROPERTIES: Color dark green, gray green, yellowish green. Luster greasy to earthy. Cleavage basal. H. about 2; G. variable, 2.508–2.572, principally 2.555. Cleavage micaceous, structure scaly. Biaxial, negative. 2V variable from 0° to 90° (due to distortion of the plates), n generally variable, mean values $\alpha = 1.559$, $\beta = 1.581$, $\gamma = 1.586$. Pleochroism distinct, X = pale yellowish green; $Y = Z$ = yellow green, herb green, emerald green. Bx_a is normal to the plane of cleavage. Birefringence = 0.027.

OCCURRENCE: Found as veinlets and ribands in the sandstones of the Klódka quarry, near Skole, eastern Carpathians, Poland.

W. F. FOSHAG

Cayeuxite

ZBIGNIEW SUJKOWSKI: The nickel bearing shales in Carpathian Flysch. *Arch. Mineral. Warsaw*, vol. **12**, pp. 118–138, 1936. Polish; English summary.

Nodules occurring in Flysch shales of Lower Cretaceous age carry carbonate, sulfide and manganese nodules. One type of nodule is called cayeuxite, in honor of Professor L. Cayeux. A typical cayeuxite nodule has the following composition: SiO_2 15.36; S 10.17; As 13.42; Sb 21.61; Fe 16.76; Ge 5.85; Al_2O_3 1.22; Cr_2O_3 0.18; MoO 1.20; NiO 0.87; CoO large traces; ZnO 0.40; MnO 0.08; MgO 1.95; CaO traces; P_2O_5 0.12; CO_2 1.60; loss at 110°C. 2.76.

W. F. F.

Thioelaterite

BOLESLAW LUDWIK DUNICZ: On thioelaterite from Bolivia. *Arch. Mineral. Warsaw*, vol. **12**, pp. 90–95, 1936. Polish, with French summary.

NAME: In allusion to its nature, an elaterite containing thioalcohols and thioethers.

CHEMICAL PROPERTIES: Analysis: C 82.27, H 12.35, N+O 1.69, Ash 0.73.

PHYSICAL PROPERTIES: Color brown, luster greasy on fresh surface, elastic. Isotropic, amorphous. G=0.989.

OCCURRENCE: Found in the San Carlos silver-tin vein, Gallofa Mine, Colquechaca, Bolivia, associated with galena, tetrahedrite, cassiterite, pyrite, marcasite, barite and quartz.

W. F. F.

Stibio-microlite

P. QUENSEL AND THELMA BERGGREN: Minerals of the Varuträsk pegmatite. XI. The niobate-tantalate group. *Geol. Fören Förh. Stockholm*, vol. **60**, pp. 216–221, 1938.

O. ROSÉN AND A. WESTGREN: Minerals of the Varuträsk pegmatite. XII. On the structure and composition of minerals belonging to the pyrochlore-atopite group and an *x*-ray analysis of disintegrated stibio-microlite. *Ibid.*, pp. 226–235.

Material from the Varuträsk pegmatite with the composition: Sb_2O_3 25.3, Ta_2O_5 52.3, Nb_2O_5 11.8, CaO 5.32, Na_2O 1.50, H_2O+ 1.11, H_2O- 0.16, SiO_2 1.38, Bi_2O_3 0.10, Al_2O_3 0.50, Fe_2O_3 0.26, MnO 0.08, TiO_2, ZrO_2, MgO, K_2O, As_2O_3, Pb, Cu, U, Y, etc., none, sum 99.81, is shown to consist of stibio-tantalite and an isotropic mineral, with minor amounts of native antimony and cervantite. Since the material shows evidence of being derived from a pre-existing mineral, the analysis is calculated to (Sb, Ca) (Ta, Nb) $(O, OH)_4$ as the formula of the original mineral. This mineral, as yet known only in the disintegrated state, is called stibio-microlite.

W. F. F.

Soda-Killinite

P. QUENSEL: Minerals of the Varuträsk Pegmatite. X. Spodumene and its alteration products. *Ibid.*, vol. **60**, pp. 201–215, 1938.

Killinite is used as a general term for a heterogeneous hypogene alteration product of spodumene, consisting principally of a mixture of several minerals of the kaolin group and a micaceous mineral. The Varuträsk "killinite," because of its high soda content is termed soda-killinite and consists of a problematic secondary Na-spodumene, cimolite, halloysite and illite.

W. F. F.